

THE NOVOCASTRA™ JOURNAL OF HISTOPATHOLOGY

reAGENTS

- 05** Validation Trial of the Bond Polymer Refine Red Detection™ System
- 13** Hypoxia-inducible Gene 2 (HIG2) Protein: New Frontiers in Diagnosis, Prognosis and Targeted Treatment of Renal Cell Carcinoma
- 20** 3D Histopathology of the Liver Using Dual Chromogen Histochemistry
- 26** Automated Double Immunoenzymatic and Colorimetric In-Situ Hybridization Techniques in Evaluation of Immunoglobulin Light Chain Expression

Guidelines for Authors

Scope

To cover all areas of histopathology, including molecular techniques, immunohistochemistry and histology. Our objective is to provide a medium for people to publish scientifically robust articles where they have used our reagents and instrumentation. We will publish both full papers as well as short communications.

Suitable subjects

The papers can cover the use of any of our products or services from reagents to instrumentation. We would look to have novel material investigating the benefits of these products.

Where looking at primary antibodies, we will ask only that comparisons be made to our own product line, for example using our detection systems and ancillaries. Where this is impractical the paper should discuss the utility and quality of the product and may compare directly to our competitors products where appropriate.

Project management

Leica Microsystems will assign a liaison manager to paper. This person will be responsible for coordinating and managing all communications with the author. A Leica Microsystems scientific expert may be assigned to oversee a project.

Document release

Both the laboratory and Leica Microsystems must formally approve any document arising from a collaboration before it is released.

Document format and style guide

Document preparation

All documents should be in English, well presented and laid out with all grammar and punctuation checked. Language and terms must be consistent (eg all US English or all UK English). All abbreviations, figure references and terminology must remain consistent throughout the manuscript. All acronyms must be spelt out initially with the acronym in parenthesis, eg turnaround time (TAT). This need not apply for commonly understood acronyms, eg IHC. Abbreviations should be followed by the words for which they stand initially. Thereafter the abbreviation can be used freely.

To help authors maintain consistency and good style, we have developed a style guide that we recommend all authors refer to. Please email us for a copy.

Document layout

The document should flow as follows:

1. The title should be succinct and followed on the subsequent line by the authors. Authors are to be listed by first name and surname, department, institute, city ZIP or postal code followed by country.
2. The abstract, which should be a comprehensive overview not exceed 400 words.
3. Introduction.
4. Method and materials.
5. Results.
6. Discussion.
7. Conclusion.

For review articles, subheadings and sections will vary depending on the nature of the subject covered. In these cases it is assumed that the appropriate subheadings will be chosen in a logical fashion.

References

Each author is responsible for the accuracy of references. References to websites should be avoided where possible, but if used should cite the date they were accessed. Personal communications should be avoided where possible also.

Format: Vancouver style

See below for example:

1. Bennett GL, Horuk R. Iodination of chemokines for use in receptor binding analysis. In: Horuk R, editor. Chemokine receptors. New York: Academic Press; 1997. p. 134-48. (Methods in Enzymology; vol 288).
2. Coffee drinking and cancer of the pancreas [editorial]. BMJ 1981;283:628.

For more detailed information, you can visit the website at

<http://www.library.uq.edu.au/training/citation/vancouv.pdf>

Figures

Figures, including all diagrams, charts and illustrations should all be labelled sequentially, numbered and referred to where applicable in the body of text. Figure references within the main text should not be abbreviated to Fig.

Tables

Tables should be numbered sequentially as Table 1, Table 2 as with figures and be referred to as such in the main body of text.

Illustrations

Images are required as 35 mm slides or an electronic version in a high resolution format (300 dpi). Eg JPEG, TIF or EPS. Drawings and charts should be provided in a graphics program such as Adobe Illustrator, PhotoShop, Corel or Freehand. We cannot use images from Word or Powerpoint.

Submission

The length of the documents will vary from case to case but as a rule:

- Doubled-spaced, 12-point type.
- Text format: A hard copy plus an electronic copy in a common editing program (eg Microsoft Word). Acrobat documents are acceptable so long as they are not protected and the text is selectable. PowerPoint documents are not acceptable.
- Image format: Approximately 5-10 images per article are preferred (including photographs, tables, graphs, schematics etc.) - No PowerPoint documents please.

They should be emailed to reagents@leica-microsystems.com or copied to a disk and mailed to:

reAGENTS

Leica Biosystems Newcastle Ltd, Balliol Business Park, Benton Lane
Newcastle upon Tyne, NE12 8EW, United Kingdom

Document distribution and use

This document will be published in the reAGENTS Journal, however, it will be subject to other purposes. By submitting this document for publication you are agreeing to any of the listed uses below:

- Leica Microsystems has the right to print and distribute an unlimited number of copies of the document;
- the document may be distributed in a printed format or in an electronic format that cannot be altered (eg as a locked pdf);
- Leica Microsystems will supply the laboratory with an electronic copy of the document and as many high-quality printed copies as they require;
- the document must not be altered in any way by either Leica Microsystems or the laboratory without formal approval by both parties;

For more information regarding in-house style and guidelines please email

reagents@leica-microsystems.com

Immunohistochemistry and Molecular Testing's Co-Evolving Roles

Colin Tristram, Innovations Manager

Leica Biosystems Newcastle Ltd

As molecular techniques become routine throughout all Pathology disciplines, we reflect on the role of traditional IHC and its use in current and future diagnostic protocols.

The routine use of IHC has never been greater or more widespread. The overall market for IHC antibodies and reagents continues to grow, outpacing almost all pathology disciplines. Sadly, this correlates to the increase in the rates of cancer globally. At Leica, our business growth is fuelled by testing volumes, and the continuous release of clinically validated antibodies providing better diagnosis and therapy prediction, not to mention an increase in their application in clinical research.

The possibility remains that one day molecular applications, including many based on the Polymerase Chain Reaction (PCR), may replace some routine IHC tests. Gene profiling of tumours offers the potential to completely characterise the patient sample to more thoroughly classify cancers and provide both prognostic and predictive data for better patient management.

PCR based tests can provide prognostic data

Some PCR based tests provide complex prognostic data, particularly in breast cancer. While the data is useful, there is debate amongst pathologists whether this data is truly better than that already provided by existing methods such as the Nottingham Prognostic Index, derived from routinely assessed pathological factors on H&E stained sections. One factor that all can agree on is that the latter is significantly more economical.

There are also PCR based tests entering routine histopathology laboratories for the detection of somatic tumour mutations such as K-Ras, in the setting of colon and lung cancer. While theranostic in nature, its utility has driven the uptake of PCR methodology in laboratories that previously never provided PCR testing as a clinical service. There are a number of commercial tests available for this assessment and most of them have proven comparable to sequencing. A key issue with all such tests, especially when offered by laboratories with no track record in molecular pathology, is a definite requirement for thorough quality assurance.¹

In-situ hybridisation can provide data within the context of tissue morphology

In-situ hybridisation (ISH) as a molecular application is already widely adopted in histopathology laboratories. With ISH, one can appreciate the targets directly in relation to histology and morphology, at least with chromogenic formats, which provides greater context regarding the target and the associated pathology. This therefore lends itself to histopathology far more easily than expression profiling or PCR. Even fluorescent in-situ hybridisation, while not necessarily being able to view the target directly in relation to the tumour and surrounding tissue, still provides the “gold standard” in many assessments such as Her2.

PCR has advantages where antibodies have been difficult to develop

This desire to see abnormalities in context has led to many requests for a monoclonal antibody to K-Ras mutations. However, point mutations within the variable codons resulting in ever so subtle amino acid substitutions make it difficult to develop antibodies, regardless of species, that are sufficiently sensitive. Here applications such as PCR have a distinct advantage. One of the few ways to circumvent this is to detect surrogate markers that are consistently detectable in the presence of mutations, alas this is not always achievable.

Cases where immunohistochemistry has allowed PCR to be supplanted

But let's consider previous PCR-based evaluations such as that of mismatch repair markers, MLH1, MSH2, MSH6 and PMS2. These were, up until approximately ten years ago, largely restricted to PCR-based microsatellite instability (MSI) analysis, until reliable and robust monoclonal antibodies were made available. Leica have just released PMS2 to complete our range of antibodies for the analysis of tumours possibly related to Lynch syndrome (Hereditary Non-Polyposis Colorectal Cancer, HNPCC). Pathologists were quick to switch to IHC for investigation of possible Lynch syndrome because it allows one to look at these abnormalities in context and in relation to the tumour and surrounding tissue, in positive cases identifying the likely causative gene and providing vital information for subsequent germline mutation screening. Most importantly, the test employed a technique already familiar to pathology laboratories, IHC.

IHC and PCR are complementary approaches rather than replacements

Given the current technologies and utilities available, we can confidently predict a long life for IHC. We shouldn't forget that most diagnoses are still made on H&E examination alone. However, IHC comes into its own when confirming and/or refining a cancer diagnosis, with respect to prognostic or predictive information, more accurately classifying, or suggesting a likely primary tumour site. Selected molecular techniques have the capability of complimenting routine applications including IHC in cases where perhaps interpretation is difficult or that the targets are highly mutated. Examining either tumour DNA or RNA is not guaranteed to reflect protein expression and therefore phenotype. As most, if not all, drugs target these proteins it is sometimes important to be looking at protein not only for diagnosis but also for therapeutic decisions. The pathologist's overriding need to observe the morphology of the tumour and protein expression is likely to remain.

Reference

1. Oliner K, Juan T, Suggs S, et al. A comparability study of 5 commercial K-Ras tests. *Diagn Pathol.* 2010 Apr 16;5(1):23.

Front cover image: H1G2, clone HX34Y, on clear cell carcinoma x400 original magnification.

Contents

- 05 Validation Trial of the Bond Polymer Refine Red Detection™ System**
Anagnostopoulos I
- 08 A Full Immunohistochemical Evaluation of a Novel Monoclonal Antibody to Folate Receptor - alpha (FR-α)**
Scorer P, Lawson N, and Quinn A
- 13 Hypoxia-Inducible Gene 2 (HIG2) Protein: New Frontiers in Diagnosis, Prognosis and Targeted Treatment of Renal Cell Carcinoma**
Tretiakova MS and Al-Ahmadie HA
- 17 Prospective Evaluation of New CD19, CD30 and CD7 Antibodies for Fixed Tissue Immunohistology**
Wilkins BS, Menon G, Cowell S, Hall M, Piggott NH, Scorer P, Tristram C and McIntosh G
- 20 3D Histopathology of the Liver Using Dual Chromogen Histochemistry**
Ismail A, Gray S, Jackson P, Shires M, Crellin DM, Magee D, Quirke P and Treanor D
- 23 Immunohistochemical Analysis of Carbonic Anhydrase IX (CA IX) in Renal Cortical Tumors**
Illei PB
- 26 Automated Double Immunoenzymatic and Colorimetric In-Situ Hybridization Techniques in Evaluation of Immunoglobulin Light Chain Expression**
Webber BA and Cohen C
- 30 CD99: Development and Evaluation of a Novel Monoclonal Antibody for Use in Manual and Automated Immunohistochemistry**
Cleghorn A, Lee MJS, Doherty J, Lawson N, Walker JN, Piggott NH, Scorer PW, Pinkney M, McIntosh G
- 35 R&D Reflections**
McIntosh G

Validation Trial of the Bond Polymer Refine Red Detection™ System

Anagnostopoulos I

Department of Pathology, Charité Medical University Berlin, Campus Mitte, Berlin, Germany

Abstract

Here we describe the assessment of a new alkaline phosphatase-based detection system developed by Leica Biosystems Ltd. Bond Polymer Refine Red Detection, for use on the Bond automated system, was assessed with in excess of 50 antibodies in tandem with the Ventana BenchMark® XT and ultraView™ Universal Alkaline Phosphatase Red Detection Kit. Three hundred and fifty slides were assessed, with Bond Polymer Refine Red Detection giving comparable or superior results in all instances. The new red detection system is a welcome addition to the laboratory for routine diagnostic work.

Introduction

Immunohistochemistry using alkaline phosphatase (AP)-based detection systems have been used for many years.¹ Red precipitation is advantageous in many settings in particular for dermatopathology where melanin pigmentation can obscure or make interpretation of brown precipitate of peroxidase-based detection systems more demanding.

It is also useful especially in tissue specimens where endogenous peroxidase reactivity can cause background interference. (A further useful application are double labellings employing brown and red detection systems for simultaneous visualisation of different antigens on the same tissue sections).

Due to the contrast of red against the blue of hematoxylin some pathologists and laboratories run AP-based detection systems on all routine immunohistochemistry. This is common in central Europe in particular Germany.

The need for in-vitro Diagnostic (IVD) classified products has become more apparent with the sophistication of the technology now employed in laboratories, where instrumentation is taking over much of the work that was done by hand. IVD labelled products provide the user with more confidence in their application. While not true for all companies, many leading suppliers put as much work and effort into the validation of their research use only formats as they do for their IVD products.

However, in light of these requirements Leica Biosystems have developed an IVD labelled Bond Polymer Refine Red Detection (DS9390).

This article demonstrates some of the studies and assessments performed at the Department of Pathology, Charité Medical University Berlin, Campus Mitte as part of a wider multicenter validation study for this product.

Study design

The aim of this study has been the validation of the performance of Bond Polymer Refine Red Detection (DS9390) in the diagnostic routine of a Department of Pathology. For this purpose at least 300 slides with appropriate tissue specimens were immunostained on the Bond automated system using Bond Polymer Refine Red Detection.

In parallel, serial slides of the same tissue specimens were stained on the Ventana Benchmark XT immunostainer employing the Ventana ultraView™ Universal Alkaline Phosphatase Red Detection kit.

Table 1. Antibodies

The following antibodies were used in this study:

Antigen	Clone	Supplier
Pan - cytokeratin	MNF116	Dako
HMW Cytokeratin	CK34BE12	Dako
Cytokeratins 5/6	D5/16B4	Zytomed
Cytokeratin 5	XM26	Leica (Novocastra)
Cytokeratin 7	OV-TL12/30	Dako
Cytokeratin 14	LL002	BioGenex
Cytokeratin 20	KS20.8	Dako
Smooth Muscle Actin	1A4	Dako
Desmin	De33	Dako
Synaptophysin	2ZG12	Leica (Novocastra)
Chromogranin	LK2H10	BioGenex
Estrogen Receptor	SP1	NeoMarkers
Progesterone Receptor	PgR636	Dako
p63	4A4	Santa Cruz
HMB45	HMB45	Dako
MelanA	A103	Dako
S-100	15E2E2	BioGenex
CD20	L26	Dako
CD3	Polyclonal	Dako
CD3	LN10	Leica (Novocastra)
CD5	CD5/54/B4	Leica (Novocastra)
CD4	1F6	Leica (Novocastra)
CD8	C8/144B	Dako
CD10	56C6	Leica (Novocastra)
Cyclin D1	P2D11F11	Leica (Novocastra)
CD21	1F8	Dako
CD30	BerH2	Dako
CD68	PGM1	Dako
Kappa	Polyclonal	Dako
Lambda	Polyclonal	Dako
CD33	PWS44	Leica (Novocastra)

Table 1. Antibodies (continued)

CD34	QBEnd10	Dako
CD43	DFT1	Dako
CD117	Polyclonal	Zytomed
Ki67	MIB1	Dako
Ki67	MM1	Leica (Novocastra)
BCL-2	124	Dako
BCL-6	PG-B6p	Dako
MUM1/IRF4	MUM1p	Dako
TdT	Polyclonal	Dako
Vimentin	V9	Dako
PAX5	Polyclonal	Zytomed
alpha-Fetoprotein	ZSA06	Zytomed
βHCG	M94138	BioGenex
Placental Alkaline Phosphatase	PL8-F6	BioGenex
TTF1	8G7G3/1	Zytomed
CDX2	CDX2-88	BioGenex
CA19-9	116-NS-19-9	Signet
PSA	ErPr8	BioGenex
AMACR	13H4	Biologo
Inhibin	Polyclonal	Zytomed
CD99	12E7	Dako
Perforin	5B10	Leica (Novocastra)

Material and Methods

Tissue specimens

Paraffin embedded sections from tissue specimens of 57 patients were employed in this study. All cases had been referred to the Department of Pathology, Charité Medical University Berlin, Campus Mitte. In all cases an immunohistochemical analysis has been necessary in order to:

1. Establish the diagnosis of a malignant tumour and perform a precise classification
2. Evaluate the tumour stage
3. Identify pre-neoplastic conditions, and
4. Evaluate tumour features important for therapeutic decisions (i.e. steroid hormone receptor expression, determination of the growth fraction).

In particular, among the cases investigated there were 12 cases with breast cancer and accompanying intraductal proliferative lesions, 10 cases of enlarged lymph nodes with reactive and neoplastic conditions, 4 cases of malignant melanoma with extensive lymphadenectomy, 6 cases with germinal and epithelial tumours of the ovary and testis, 4 cases with primary and metastatic lung tumours, 4 cases with prostatic core biopsies, 3 cases with undifferentiated carcinoma of unknown primary, 2 cases with gastrointestinal stoma tumours and other more rare cases including tumours of the thymus, and of soft tissue.

In all cases selected there was sufficient material available in order to perform the parallel immunostains on the Bond automated system and Ventana BenchMark® XT.

From the paraffin blocks selected for immunohistochemical analysis serial tissue sections at approximately 3 µm thickness were cut and further processed in the automated immunostainers.

The applied antibody concentration and the appropriate antigen retrieval protocols had been established in the Ventana BenchMark® XT for the daily diagnostic routine. The specific immunostain for each of these antibodies was additionally evaluated using on-slide controls. Depending on the antibody applied, these on-slide controls consisted either of a multi-tissue array containing lung, thyroid, skin, ureter, melanoma, ovarian carcinoma, placenta, pancreas and carcinoma of the prostate or of appendix cross sections containing mucosa, activated lymphoid tissue, and muscular wall.

Data collection

All slides were evaluated by an experienced pathologist who had to decide whether the immunostain obtained employing the Bond Polymer Refine Red Detection was acceptable for diagnostic purposes or not.

In addition he had to evaluate in parallel the immunostains obtained using the Ventana ultraView™ Universal Alkaline Phosphatase Red Detection kit and verify whether the performance of both kits was similar, superior or inferior when directly compared to each other.

The results were recorded on an evaluation sheet and discussed during a weekly telephone conference.

Results

A total of 350 slides have been stained during this study using Bond Polymer Refine Red Detection. In all instances the immunostain has been found to be acceptable for diagnostic purposes (Figure 1 and 2). Neither disturbing precipitates nor unspecific stains have been observed. In most instances the performance of the Bond Polymer Refine Red Detection was equal to that of the Ventana equivalent.

However, on 39 occasions the Bond Polymer Refine Red Detection delivered a crisper, more intensive immunostain, whilst in no instance was an inferior result observed. In addition, there was no interference between the red reaction product (S-100 protein) and the melanin granules in a case of malignant melanoma (Figure 3).

Conclusion

The results of our assessment have indicated that Bond Polymer Refine Red Detection is suitable for use in routine diagnostic immunohistochemistry on the Bond automated system. This new detection system provides an intensity and sharpness of staining that will facilitate the introduction of double-staining protocols into routine automated immunohistochemical staining.

References

1. Cordell JL, Falini B, Erber WN, et al. Immunoenzymatic labeling of monoclonal antibodies using immune complexes of alkaline phosphatase and monoclonal anti-alkaline phosphatase (APAAP complexes). *J Histochem Cytochem* 1984;32(2):219-29.

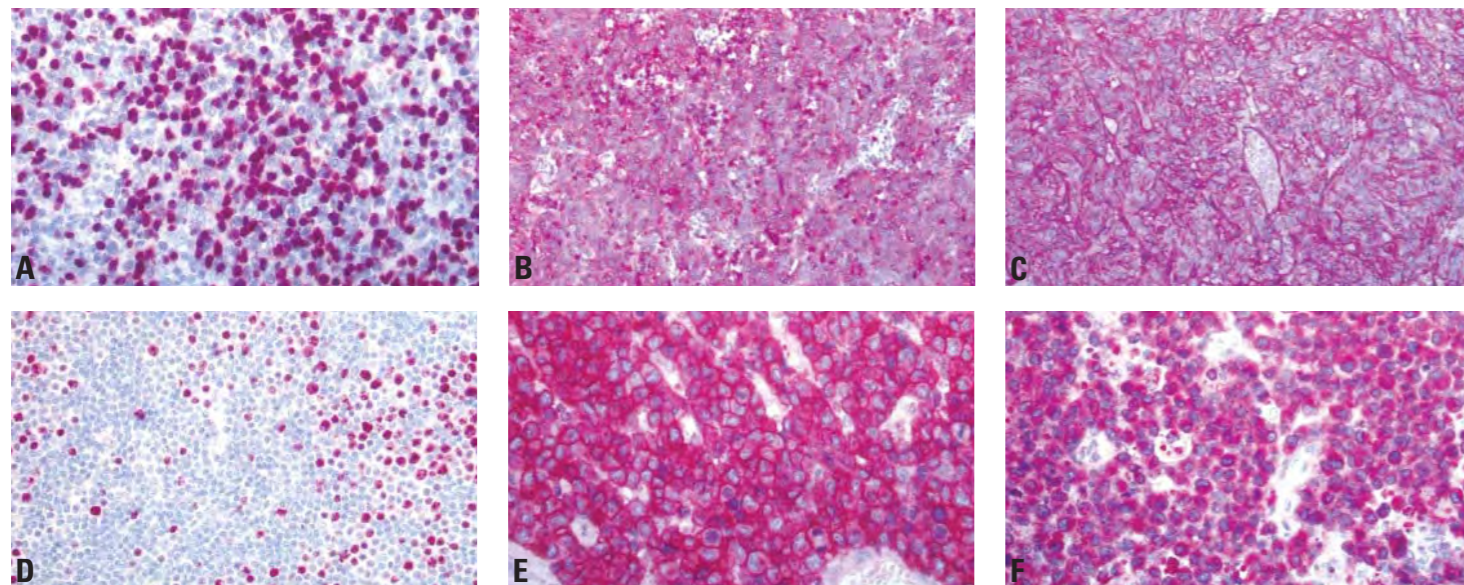


Figure 1. Automated immunohistochemical staining of formalin-fixed, paraffin-embedded tissue sections using Bond Polymer Refine Red Detection.

- A. Demonstration of non-neoplastic thymocytes expressing TdT in a thymoma.
- B. Detection of CD5 in a case of a carcinoma with thymus-like differentiation.
- C. CD34 in a case of gastrointestinal stromal tumour (GIST).
- D. Ki-67 in a case of a low grade B cell lymphoma.
- E. All tumour cells of an anaplastic large cell lymphoma exhibit an intense CD30 expression.
- F. Demonstration of the cytotoxic molecule perforin in the tumour cells of the anaplastic large cell lymphoma.

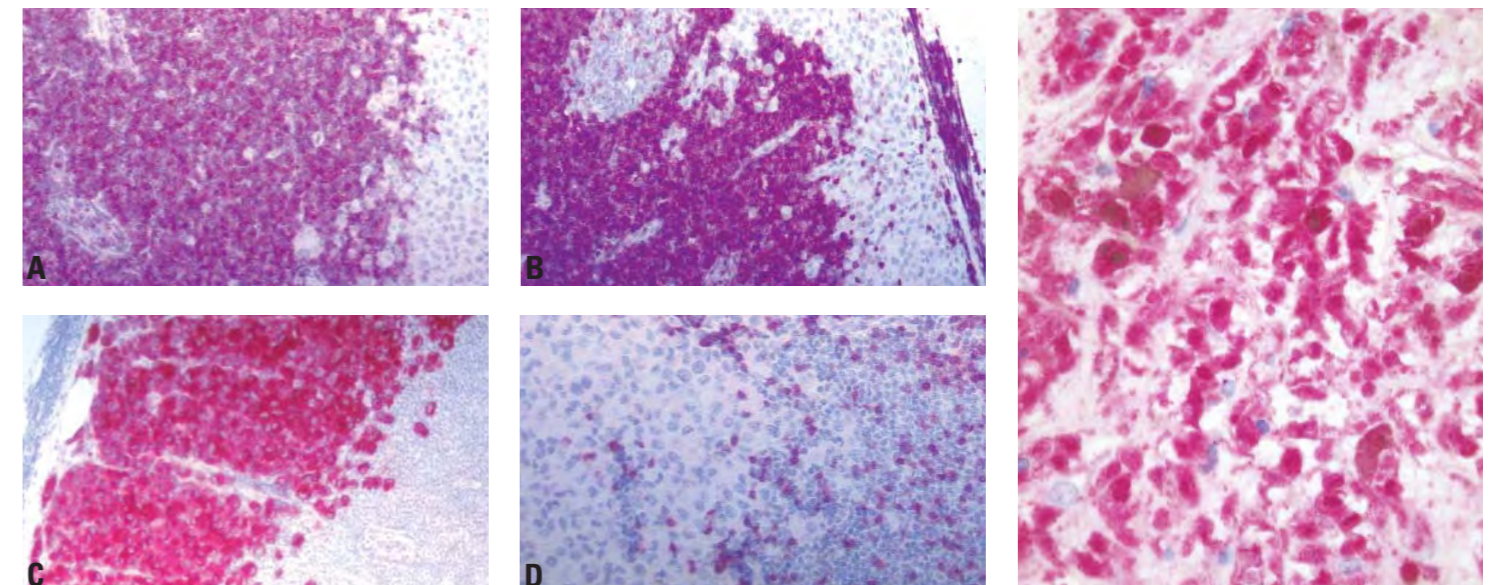


Figure 2. Lymph node with simultaneous manifestation of a chronic lymphocytic leukemia expressing CD23 (A), CD5 (B) and of a metastasis of a malignant melanoma (Melan A expression; C). Few intermingled T cells expressing CD3 (D). Automated immunohistochemical staining using Bond Polymer Refine Red Detection.

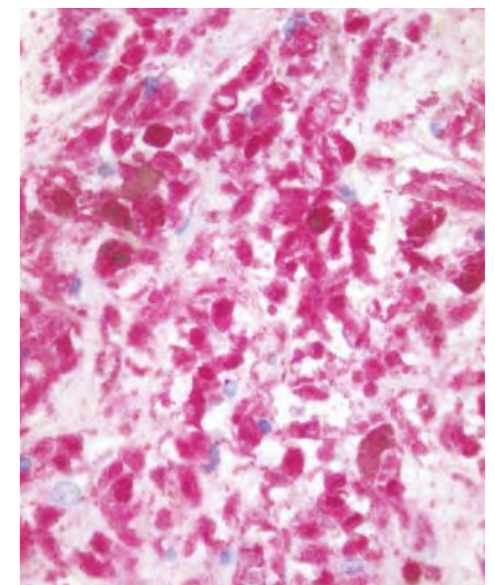


Figure 3. Automated immunohistochemical staining for S100 on a case of malignant melanoma using Bond Polymer Refine Red Detection.

A Full Immunohistochemical Evaluation of a Novel Monoclonal Antibody to Folate Receptor - alpha (FR- α)

Scorer P, Lawson N and Quinn A

Leica Biosystems Newcastle, Balliol Business Park, Benton Lane, Newcastle upon Tyne, UK

Abstract

Folate Receptor – alpha (FR- α) has been described extensively in many tumour and tissue types. Up to now the majority of this work has been looking at mRNA with some limited immunohistochemistry restricted to frozen tissue. In this article we review the extensive testing undertaken to evaluate a novel mouse monoclonal antibody to FR- α that works in formalin-fixed paraffin-embedded tissue. The development of this antibody opens up the potential for the wider clinical community to study and possibly establish its utility as a diagnostic tool. In light of pharmaceutical approaches to FR- α , this target may yet be employed in the identification of patients suitable for treatment. Our findings indicate that FR- α is most prevalent in ovarian cancers, with additional expression observed in tissues such as kidney, lung and endometrial cancers, all of which may be of interest to clinicians.

Introduction

Folate Receptor - alpha (FR- α) is a member of the FOLR gene family of glycopolypeptides with a high affinity for circulating physiological folates. FR- α is attached to the plasma membrane by a glycoposphatidyl inositol (GPI) anchor and transports folates involving a mechanism termed potocytosis, where folate-receptor complexes are internalised and the receptor is 'recycled' back to the cell membrane. Immunohistochemical (IHC) reactivity observed may be both membrane and cytoplasmic due to this mechanism.^{1,2,3} To date few antibodies suitable for use on formalin-fixed, paraffin-embedded tissue are commercially available and much data on FR- α tissue expression has been elucidated by the use of the MOv18 antibody, suitable for use on frozen tissue sections only. Here we describe the full immunohistochemical evaluation of a monoclonal antibody to FR- α (clone BN3.2).⁴

Materials and Methods

Immunohistochemistry (IHC) was performed on formalin-fixed, paraffin-embedded tissues sections using the Novocastra™ antibody to FR- α (clone BN3.2). Clone BN3.2 was optimised for both manual and automated Bond™ system use, and evaluated on normal and tumour tissues. Manual assessment was carried out using pressure cooker epitope retrieval with Novocastra Epitope Retrieval Solution pH6 (RE7113), incubation with clone BN3.2 (1:100) for 30 minutes and visualised using the Novolink Polymer Detection System (RE7140-K). Using the automated Bond system, epitope retrieval was carried out using ER2 (AR9640) (pH9) retrieval solution for 20 minutes, incubation with clone BN3.2 (1:40) for 15 minutes.

The detection kit used was the Bond Polymer Refine Detection (DS9800), incubation with post primary for 8 minutes, polymer for 8 minutes, DAB for 10 minutes and Haematoxylin for 5 minutes. Positive staining was classified as positive FR- α staining of any intensity, in tumour tissues FR- α staining had to be present in the tumour cells to be classed as positive.

Results

IHC staining with FR- α (clone BN3.2) on formalin-fixed, paraffin-embedded tissues is summarised in Tables 1-10 and shown in Figures 1-10. The results include all negative staining results as well as positive to provide a full picture of the antibodies staining characteristics.

Normal Tissues

Normal Tissue	FR- α Staining Pattern	Normal Tissue	FR- α Staining Pattern
Colon	Negative	Lymph Node	Negative
Appendix	Negative	Thymus	Negative
Small Bowel	Negative	Tonsil	Negative
Stomach	Negative	Bone Marrow	Negative
Oesophagus	Negative	Breast	Negative
Salivary Gland	Negative	Cervix	Negative
Liver	Negative	Myometrium	Negative
Spleen	Negative	Endometrium	Negative
Ureter	Negative	Ovary	Negative
Adrenal	Negative	Skeletal Muscle	Negative
Thyroid	Negative	Smooth Muscle	Negative
Parathyroid	Negative	Heart	Negative
Pituitary	Negative	Mesothelium	Negative
Skin	Negative	Cerebellum	Negative

Normal Tissue	FR- α Staining Pattern
Kidney	Membrane/cytoplasmic staining of proximal tubules (15/17) * (Figure 1A)
Placenta	Membrane/cytoplasmic staining of trophoblasts (7/8) *
Lung	Membrane staining of luminal surfaces of bronchiolar epithelium, type II pneumocytes, alveolar membrane, submucosal glands of bronchus (25/55) * (Figure 1B)
Fallopian Tube	Moderate membrane/cytoplasmic staining of the glycocalyx of tubular epithelium
Pancreas	Weak membrane staining of ductal epithelium
Testis	Weak membrane staining of tubules

* Kidney, placenta and lung did not exhibit FR- α expression in all cases and staining intensity varied from strong to weak. Potentially due to tissue fixation as well as FR- α expression levels.

Table 1. FR- α expression in Normal Tissues (n=104).

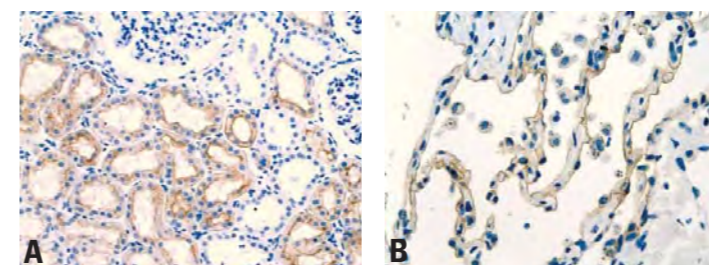


Figure 1. FR- α staining in (A) proximal tubules of normal kidney (B) alveoli of normal lung. Paraffin section (original magnification (A) x200 (B) x400).

Tumour Tissues

Cancer Type	Positive Cases
Mesotheliomas	2 / 19
Kidney Cancers	16 / 97
Ovarian Cancers	41 / 112
Colon Cancers	5 / 113
Breast Cancers	4 / 106
Endometrial Cancers	28 / 72
Lung Cancers	42 / 149
Uterine Cancers	3 / 21

Table 2. FR- α staining in tumours (n=689).

Mesotheliomas

Mesothelioma (n=19)	FR- α Staining Pattern
Epithelioid Type	strong membrane staining of tumour cells (2/12) (Figure 2)
Mixed Type	negative (0/4)
Spindle cell Type	negative (0/3)

Table 3. FR- α staining in mesothelioma.

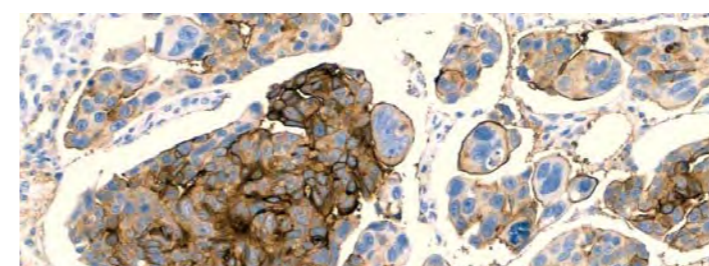


Figure 2. FR- α : moderate membrane staining in clear cell RCC. Paraffin section. (original magnification x400).

Kidney Cancers

Kidney Cancers (n=97)	FR- α Staining Pattern
Clear Cell Renal Cell Carcinoma	Weak to moderate membrane/cytoplasmic staining of tumour (16/67) (Figure 3)
Papillary Renal Cell Carcinoma	Negative (0/4)
Chromophobe Renal Cell Carcinoma	Negative (0/4)
Sarcomatoid Renal Cell Carcinoma	Negative (0/3)
Oncocytoma	Negative (0/3)
Angiomyolipoma	Negative (0/3)
Wilm's Tumour	Negative (0/3)
Urothelial Carcinoma	Negative (0/3)
Transitional Cell Carcinoma	Negative (0/7)

Table 4. FR- α staining in kidney cancers.

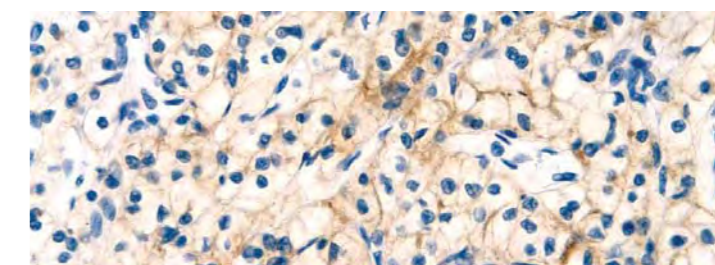


Figure 3. FR- α : moderate membrane staining in clear cell RCC. Paraffin section. (original magnification x400).

Ovarian Cancers

Ovarian Cancers (n=112)	FR- α Staining Pattern
Serous Papillary Adenocarcinoma	Strong to moderate membrane / cytoplasmic staining of tumour (27/38) * (Figure 4 & 5)
Serous Cystadenocarcinoma	Strong to moderate membrane / cytoplasmic staining of tumour (1/1)
Serous Cystadenoma	Strong to moderate membrane / cytoplasmic staining of tumour (4/11)
Serous Papillary Cystadenoma	Strong to moderate membrane / cytoplasmic staining of tumour (1/2)
Mucinous Adenocarcinoma	Strong to moderate membrane / cytoplasmic staining of tumour (1/5)
Mucous Papillary Adenocarcinoma	Strong to moderate membrane / cytoplasmic staining of tumour (1/2)
Metastatic Adenocarcinoma	Strong to moderate membrane / cytoplasmic staining of tumour (2/5)
Metastatic Transitional	Strong to moderate membrane / cytoplasmic staining of tumour (2/5)
Cell Adenocarcinoma	Strong to moderate membrane / cytoplasmic staining of tumour (2/5)
Metastatic Mucinous Adenocarcinoma	Strong to moderate membrane / cytoplasmic staining of tumour (1/1)
Clear Cell Carcinoma	Strong to moderate membrane / cytoplasmic staining of tumour (1/7)
Mucinous Cystadenocarcinoma	Negative (0/1)
Mucinous Cystadenoma	Negative (0/4)
Unspecified Carcinoma	Negative (0/2)
Squamous Cell Carcinoma	Negative (0/1)
Endodermal Sinus Tumour	Negative (0/1)
Brenner Tumour	Negative (0/2)
Krukenberg Tumour	Negative (0/5)
Granular Cell Tumour	Negative (0/1)
Granulosa Tumour	Negative (0/5)
Granular Theca Cell Tumour	Negative (0/1)
Malignant Theca Cell Tumour	Negative (0/1)
Yolk Sac Tumour	Negative (0/4)
Dysgerminoma	Negative (0/5)
Fibroma	Negative (0/2)

* Staining patterns were also identifiable, a proportion of serous papillary adenocarcinoma cases displayed distinct staining of the glycocalyx or apical membrane of tumour cells and also what appear to be cytoplasmic "vacuoles" in the tumour (Figure 5).

Table 5. FR- α staining in ovarian cancers.

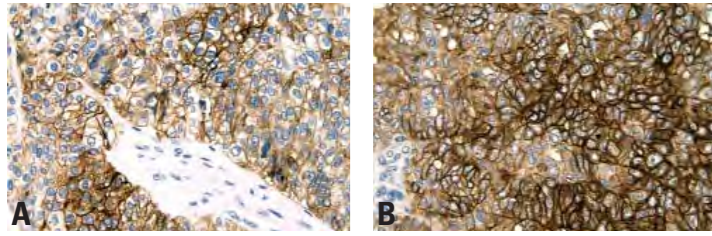


Figure 4. FR- α staining in ovarian serous papillary adenocarcinoma (A) membrane (B) membrane/cytoplasmic. (original magnification x400).

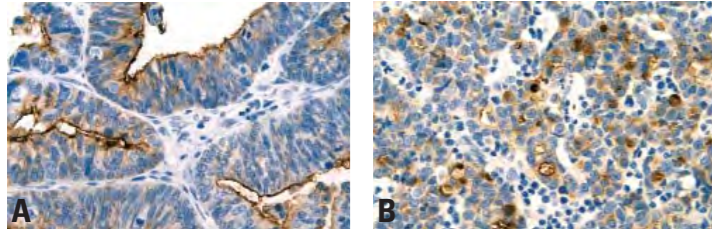


Figure 5. FR- α staining in ovarian serous papillary adenocarcinoma (A) glycocalyx staining (B) cytoplasmic "vacuole" staining. Paraffin section. (original magnification x400).

Colon Cancers

Colon Cancers (n=113)	FR- α Staining Pattern
Adenocarcinoma (Poorly Differentiated)	Strong to weak membrane/cytoplasmic staining (1/24) *
Adenocarcinoma (Moderately Differentiated)	Strong to weak membrane/cytoplasmic staining (4/67) (Figure 6)
Adenocarcinoma (Well Differentiated)	Negative (0/9)
Adenocarcinoma (Ungraded)	Negative (0/1)
Mucinous Adenocarcinoma (Poorly Differentiated)	Negative (0/5)
Mucinous Adenocarcinoma (Moderately Differentiated)	Negative (0/3)
Mucinous Adenocarcinoma (Well Differentiated)	Negative (0/4)

* A proportion of cases displayed distinct staining of the glycocalyx or apical membrane of tumour cells. In some negative tumour cases, weak staining of secreted colonic mucin was also identified.

Table 6. FR- α staining in colon cancers.

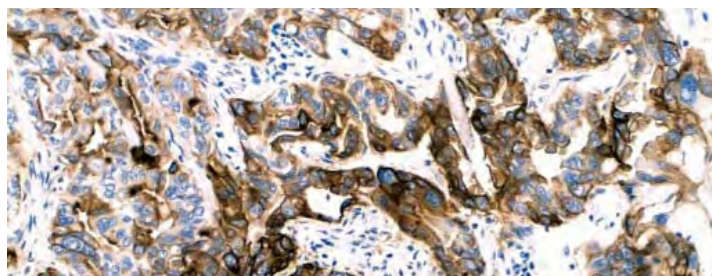


Figure 6. FR- α : strong membrane/cytoplasmic staining in moderately differentiated colonic adenocarcinoma. Paraffin section. (original magnification x200).

Breast Cancers

Breast Cancers (n=106)	FR- α Staining Pattern
Ductal Carcinoma (Moderately Differentiated)	Moderate to weak membrane staining (3/42) (Figure 7)
Lobular Carcinoma	Moderate to weak cytoplasmic staining (1/7)
Ductal Carcinoma (Poorly Differentiated)	Negative (0/31)
Ductal Carcinoma (Well Differentiated)	Negative (0/7)
Ductal Carcinoma (Ungraded)	Negative (0/7)
Ductal/Lobular Carcinoma	Negative (0/4)
Medullary Carcinoma (Ungraded)	Negative (0/8)

Table 7. FR- α staining in breast cancers.

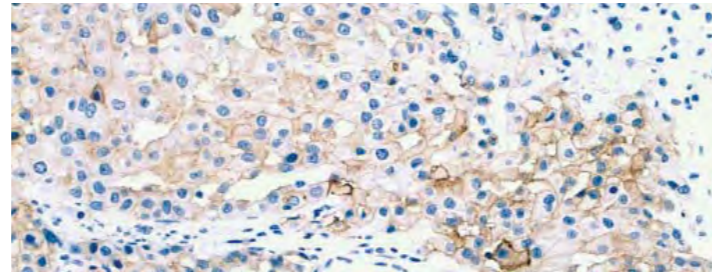


Figure 7. FR- α : moderate membrane staining in moderately differentiated infiltrating ductal carcinoma. Paraffin section. (original magnification x200).

Endometrial Cancers

Endometrial Cancers (n=72)	FR- α Staining Pattern
Endometrial Adenocarcinoma (Poorly Differentiated)	Strong to weak membrane staining (3/7)
Endometrial Adenocarcinoma (Moderately Differentiated)	Strong to weak membrane staining (12/33) * (Figure 8)
Endometrial Adenocarcinoma (Well Differentiated)	Strong to weak membrane staining (7/19)
Endometrial Adenocarcinoma (Ungraded)	Strong to weak membrane staining (5/9)
Adenosquamous Carcinoma	Weak cytoplasmic staining (1/2)
Endometrial Papillary Adenocarcinoma	Negative (0/1)
Endometrial Mixed Mullerian Tumour	Negative (0/1)

* Staining patterns were also identifiable, a proportion of cases displayed distinct staining of the glycocalyx or apical membrane of tumour cells and also what appear to be cytoplasmic "vacuoles" in the tumour.

Table 8. FR- α staining in endometrial cancers.

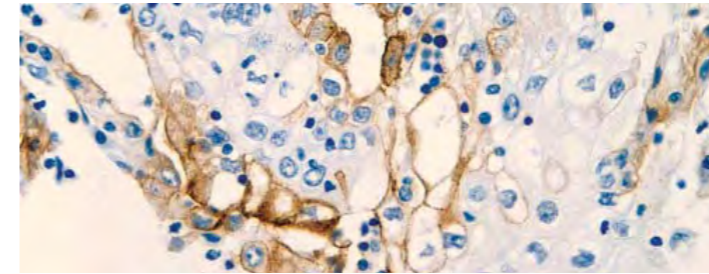


Figure 8. FR- α : strong membrane expression in moderately differentiated endometrial adenocarcinoma. Paraffin section. (original magnification x400).

Lung Cancers

Lung Cancers (n=149)	FR- α Staining Pattern
Adenocarcinoma (Poorly Differentiated)	Moderate to weak membrane/cytoplasmic staining of tumour (6/19) *
Adenocarcinoma (Moderately Differentiated)	Moderate to weak membrane/cytoplasmic staining of tumour (14/28) * (Figure 9)
Adenocarcinoma (Well Differentiated)	Moderate to weak membrane/cytoplasmic staining of tumour (6/11) *
Adenocarcinoma (Ungraded)	Moderate to weak membrane/cytoplasmic staining of tumour (6/7) *
Squamous Cell Carcinoma (Poorly Differentiated)	Moderate to weak membrane/cytoplasmic staining of tumour (1/15)
Squamous Cell Carcinoma (Moderately Differentiated)	Moderate to weak membrane/cytoplasmic staining of tumour (3/38) *
Squamous Cell Carcinoma (Well Differentiated)	Moderate to weak membrane/cytoplasmic staining of tumour (1/2) *
Adenosquamous Carcinoma (Ungraded)	Moderate to weak membrane/cytoplasmic staining of tumour (1/4)
Bronchoalveolar Carcinoma	Moderate to weak membrane/cytoplasmic staining of tumour (2/4) *
Papillary Adenocarcinoma (Moderately Differentiated)	Negative (0/4)
Small Cell Carcinoma	Negative (0/6)
Large Cell Carcinoma (Poorly Differentiated)	Negative (0/1)
Large Cell Carcinoma (Ungraded)	Negative (0/4)
Carcinoid	Negative (0/2)
Atypical Carcinoid	Negative (0/1)
Large Cell Neuroendocrine Carcinoma	Negative (0/3)

* Staining patterns were also identifiable, a proportion of cases displayed distinct staining of the glycocalyx or apical membrane of tumour cells and also what appear to be cytoplasmic "vacuoles" in the tumour.

Table 9. FR- α staining in lung cancers.

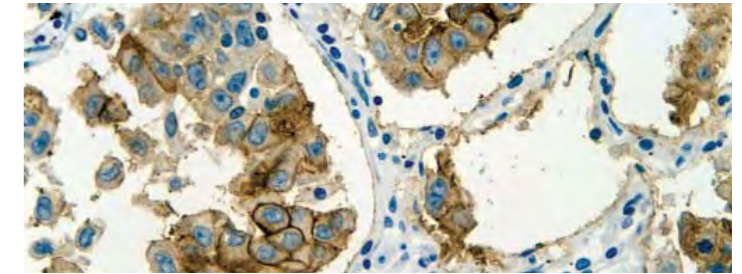


Figure 9. FR- α : strong membrane staining in a moderately differentiated lung adenocarcinoma. Paraffin section. (original magnification x400).

Uterine Cancers

Uterine Cancers (n=21)	FR- α Staining Pattern
Invasive Squamous Cell Carcinoma of Cervix	Moderate to weak membrane/cytoplasmic staining of tumour (1/5) (Figure 10)
Mucinous Adenocarcinoma of Cervix	Moderate to weak membrane/cytoplasmic staining of tumour (1/1)
Mucinous Adenocarcinoma of Cervix (Metastatic)	Moderate to weak membrane/cytoplasmic staining of tumour (1/1)
CIN 1	Negative (0/1)
CIN 2	Negative (0/2)
CIN 3	Negative (0/3)
Uterine Leiomyoma	Negative (0/2)
Uterine Leiomyosarcoma	Negative (0/1)
Uterine Adenomatoid Tumour	Negative (0/3)
Condyloma Acuminatum	Negative (0/1)
Squamous Cell Carcinoma of Vagina	Negative (0/1)

Table 10. FR- α staining in uterine cancers.

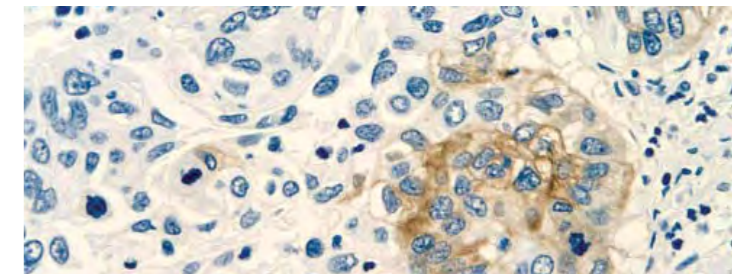


Figure 10. FR- α : moderate membrane/cytoplasmic staining in invasive squamous carcinoma of cervix. Paraffin section. (original magnification x400).

Discussion

Publications have studied the incidence of high expression of FR- α in ovarian epithelial tumours, where an increase in FR- α expression is associated with tumour progression, increased grade, and decreased survival. These studies were carried out using IHC staining on frozen tissue sections using the MOv18 and MOv19 monoclonal antibodies.^{5,6,7}

FR- α detection in formalin-fixed, paraffin-embedded tissues allows immunohistochemical studies to be carried out more extensively to determine the role of FR- α as a tumour prognostic marker and possible therapeutic target. FR- α detection has potential in a diagnostic setting as well as in translational studies incorporating clinical trials of anti-folates, such as pemetrexed, for which FR- α is believed to be potentially important in determining responsive subgroups of patients for whom targeted drug therapy would be of particular benefit.^{7,8,9,10}

FR- α is involved in the transport of folates (folic acid and its coenzymes, B vitamins) which are essential for the de novo synthesis of DNA precursors, which are imperative to survival, growth, and proliferation in both normal and tumour cells.⁴ Pemetrexed is a chemotherapy drug, chemically similar to folic acid which functions as a folate anti-metabolite and is easily transported by FR- α instead of folic acid. Substitution of pemetrexed for folic acid inhibits the formation of the DNA precursors, purine and pyrimidine nucleotides, preventing DNA and RNA formation, thus inhibiting growth and survival of both normal and cancer cells.^{11,12}

Other anti-folate therapies are also currently in the clinical trials stage. The biopharmaceutical company Morphotek are currently concluding a Phase II trial of farletuzumab, a humanised monoclonal antibody for the potential treatment of advanced ovarian cancer. The drug appears to have anti-proliferative and cytotoxic effects on tumour cells over expressing FR- α . Phase II of the trial consists of its testing as a single-agent and in combination with standard-of-care chemotherapy (carboplatin and taxane) in platinum-sensitive ovarian cancer patients experiencing their first relapse of the disease.¹³

As expected FR- α (clone BN3.2) exhibited staining in both the membrane and cytoplasm of normal tissues and tumours. Membrane staining was either complete or restricted to the apical surface (glycocalyx) in certain tissues and tumours. Glycocalyx staining was predominantly found in adenocarcinomas of endometrium, ovary and lung. Cytoplasmic “vacuole” staining within tumour cells appeared to occur mostly in adenocarcinomas of endometrium, ovary, colon and lung, these “vacuoles” are possibly small secretory inclusions containing FR- α .

FR- α staining intensity was variable, mostly weak to moderate, with the strongest expression found in ovarian serous papillary adenocarcinomas. The variations in FR- α staining intensity are more probably linked to FR- α expression than IHC protocol variability. The IHC protocols proved to be sensitive enough to pick up the low levels of FR- α found naturally in normal lung (alveoli and bronchial epithelium), normal kidney and fallopian tube.

Conclusion

As expected from the literature, FR- α staining was most prevalent in ovarian tumours. Some additional areas of interest include lung and endometrial cancers, where 47% of lung adenocarcinomas and 50% of endometrial adenocarcinomas expressed FR- α , which may be of interest to clinicians.

Interestingly in kidney cancers FR- α was only found to be expressed in a proportion (24%) of clear cell type renal cell carcinomas, which may or may not be of potential significance.

FR- α (clone BN3.2) will hopefully provide clinicians and researchers with the ability to study FR- α expression in formalin-fixed, paraffin-embedded tissues, leading to a clearer understanding of the diagnostic, prognostic and therapeutic potentials of FR- α in various cancer types.

References

1. Elnakat H, Ratnam M. Distribution, functionality and gene regulation of folate receptor isoforms: Implications in targeted therapy. *Advanced Drug Delivery Reviews* 2004;56:1067-1084.
2. Lucock M. Folic acid: Nutritional biochemistry, molecular biology and role in disease processes. *Molecular Genetics and Metabolism* 2000;71:121-138.
3. Theti DS, Jackman AL. The role of alpha-folate receptor-mediated transport in the antitumor activity of antifolate drugs. *Clinical Cancer Research* 2004;10(3):1080-1089.
4. Smith AE, Pinkney M, Piggott NH, et al. A Novel Monoclonal Antibody for Detection of Folate Receptor Alpha in Paraffin-Embedded Tissues: Hybridoma 2007;26(5):281-288.
5. Toffoli G, Cernigoi C, Russo A, et al. Overexpression of folate binding protein in ovarian cancers. *International Journal of Cancer* 1997;74:193-198.
6. Toffoli G, Russo A, Gallo A, et al. Expression of folate binding protein as a prognostic factor for response to platinum containing chemotherapy and survival in human ovarian cancer. *International Journal of Cancer* 1998;79:121-126.
7. Weitman SD, Weinberg LR, Coney LR, et al. Cellular localisation of the folate receptor potential role in drug toxicity and folate homeostasis. *Cancer Research* 1992;52:6708-6711.
8. Lu Y, Low PS. Immunotherapy of folate receptor-expressing tumours: review of recent advances and future prospects. *Journal of Controlled Release* 2003;91:17-29.
9. Mangiarotti F, Miotti S, Galmozzi E, et al. Functional effect of point mutations in the alpha folate receptor gene of CABA I ovarian carcinoma cells. *Journal of Cellular Biochemistry* 2001;81:488-498.
10. Jackman AL, Theti DS, Gibbs DD. Antifolates targeted specifically to the folate receptor. *Advanced Drug Delivery Reviews* 2004;56:1111-1125.
11. McLeod HL, Cassidy J, Powrie RH, et al. Pharmacokinetic and Pharmacodynamic Evaluation of the Glycinamide Ribonucleotide Formyltransferase Inhibitor AG2034. *Clinical Cancer Research (American Association for Cancer Research)* 2000;6:2677-2684.
12. Avendano C, Menendez JC. *Medicinal Chemistry of Anticancer Drugs*. Elsevier: Amsterdam 2008:p37.
13. Farletuzumab Data Presented on Phase II Clinical Trial in First-Relapsed Ovarian Cancer Subjects. 2009: <http://www.morphotek.com/Default.aspx?p=2573&d=376>.

Hypoxia-inducible Gene 2 (HIG2) Protein: New Frontiers in Diagnosis, Prognosis and Targeted Treatment of Renal Cell Carcinoma

Tretiakova MS^{1,2} and Al-Ahmadie² HA

1. Department of Pathology, University of Chicago, Chicago, IL, 60637, USA
2. Department of Pathology, Memorial Sloan-Kettering Cancer Center, New York, NY, 10065, USA

Background: Tumor hypoxia is a common phenomenon in some subtypes of renal cell carcinomas (RCC) and may play a role in their biology and response to treatment. Significant differences in the clinical course and behavior exist among the subtypes of RCC ranging from aggressive clear cell (CCRCC) to indolent chromophobe (ChRCC) variants underscoring the importance to make the correct diagnosis in these tumors, especially when dealing with limited material such as needle biopsy specimens. Here we evaluate a novel hypoxia marker HIG2 in renal cortical tumors and normal tissues.

Design: Tissue microarray sections containing 308 cases of CCRCC, papillary (PRCC), ChRCC, oncocytomas (ONC) and 41 normal tissues were stained with HIG2 antibody (clone HX34Y) using enzymatic digestion and Bond-max reagents. Each case was represented by three 1 mm tissue cores, for which reactivity >5% cells was considered positive. The IHC intensity was scored as weak (1), moderate (2) or strong (3). The mean value was recorded for each individual case as the average intensity of all 3 cores.

Result: HIG2 was positive in the majority of CCRCC (92%, mean value 2.14), two thirds of PRCC (67%, mean value 1.49) (p<0.01). In ChRCC and ONC, the vast majority of cases were negative for HIG2 (mean value 0.11 and 0.08 respectively, p<0.01). In normal tissues HIG2 was positive only in tubules of 1/3 of fetal kidneys and 4/8 adult kidneys showing stromal fibrosis. HIG2 in all positive cases exhibited granular cytoplasmic staining often combined with membranous accentuation.

Conclusion: Our results strongly suggest that the differential expression of HIG2 in subtypes of RCC may have a prognostic value in selecting tumor with low-oxygen resistance for further hypoxia-targeted therapies. HIG2 may be used as a diagnostic aid in CCRCC discrimination from morphologic mimickers in limited diagnostic material, and potentially in metastatic disease provided HIG2 expression is retained, which needs to be further elucidated.

Introduction

Renal cell carcinoma (RCC) represents over 90% of all adult kidney malignancies and over the past decades had shown a steady increase incidence and mortality.^{1,2} Despite high proportion of localized disease, approximately one third of patients present with advanced disease, and half of those will eventually relapse.³ Clear cell RCC, which is the most common subtype of RCC, is characterized by abnormalities in the VHL-HIF pathway in the majority of cases, has a low response rate to radiation and chemotherapy, and standard immunotherapies lead to complete response in fewer than 15% of patients.⁴⁻⁶ Recent therapeutic modalities that are based on targeting specific molecules in the oncogenic pathways, namely tyrosine kinase inhibitors, have shown promising results in early trials, especially those in advanced and metastatic disease.^{4,7} The early success in such targeted therapy made it attractive to find molecules that are preferentially expressed in subtypes of RCC with the hope that future work may identify agents that can specifically target these molecules and be added to the treatment options to patients afflicted with these tumors, especially in advanced or metastatic settings.

Clear cell RCC is well known for its intense vascularity and high dependence on hypoxia-inducible factors (HIF), playing fundamental role in malignant transformation via transcriptional regulation. Although the HIF pathway was originally linked to Von Hippel Linday (VHL)-deficient clear cell RCC, over-expression of HIF is documented in all RCC histologic subtypes.⁷ Novel therapeutic agents targeting HIF or its

transcription targets have demonstrated promising antitumor activity in multiple clinical trials.³ The clinical effort to exploit hypoxia, however, has been hindered by the failure to accurately identify patients who would benefit the most from hypoxia-targeted therapy.

The negative results of several clinical trials can be attributed to patient heterogeneity and the fact that most frequently used markers of endogenous hypoxia, like HIF-1 α and carbonic anhydrase IX (CA IX), can be influenced by VHL status, several non-hypoxic stimuli, including nitric oxide, cytokines (interleukin-1b and tumor necrosis factor α), trophic stimuli (serum, insulin, insulin-like growth factors), and oncogenes.^{8,9} Moreover, practical use of some IHC markers, like HIF-1 α , is limited in paraffin tissues due to technical pitfalls of using tyramide amplification systems, variable methodology and interpretation generating conflicting data.¹⁰ Therefore, the search for better markers or a panel of hypoxia markers for routine use on paraffin sections could significantly aid in diagnostic and prognostic studies of RCC, as well as improve patient selection for target-specific therapies.

Hypoxia-inducible gene 2 (HIG2) was first identified by Denko et al⁵ in oxygen deprived cultured human cervical epithelial cells by representational difference analysis, and later confirmed by cDNA microarray study among significantly up-regulated genes in RCC and fetal kidney.⁶ Even though exact function of HIG2 is largely unknown, there is some evidence of its essential role as a RCC growth factor highly sensitive to tumor microenvironment and targeted by Wnt/beta-catenin

signaling.^{5, 11} However, further investigations of HIG2 expression and tissue localization were impeded by lack of specific commercially available antibody. Here we evaluate a recently developed monoclonal HIG2 antibody in a large scale study of subtypes of RCC, benign oncocytomas and non-neoplastic tissues.

Material and methods

Our study group consisted of 308 nephrectomies performed at the University of Chicago Medical Center from 1992 to 2008, including 155 clear cell RCC (CCRCC), 76 papillary (PRCC), 53 chromophobe (ChRCC), 24 oncocytomas (ONC), 11 normal kidneys (including 8 adult and 3 fetal), 4 adrenal glands, 20 normal livers and 6 tonsils. H&E slides from each case were reviewed by both pathologists to select representative sections for tissue microarray (TMA) fabrication with Institutional Review Board approval. From each case a minimum of 3 tissue cylinders with a diameter of 1 or 1.5 mm were arrayed into a recipient block using either manual or automated tissue microarrayer ATA-27 (Beecher Instruments, Sun Prairie, WI). 4 µm thick serial sections were submitted for IHC analysis using mouse monoclonal antibody for HIG-2 (Novocastra™ clone HX34Y, two dilutions at 1:100 and 1:50, Leica Biosystems, Newcastle, UK). Antigen retrieval was carried by enzymatic digestion using either Proteinase K (DAKO, Carpinteria, CA) for 5 minutes or Enzyme 1 (Leica Biosystems, Newcastle, UK). Further steps were either manual, using the Envision+ detection system, (DAKO, Carpinteria, CA), or automated, using the Bond-max system (Leica Biosystems, Melbourne, Australia) with Bond Polymer Refine Detection (Leica Biosystems, Newcastle, UK). Comparison of manual and automated staining results showed similarity in staining patterns, but higher reproducibility and staining intensity with the automated method, which was applied further to all our TMA sections.

All of the slides were reviewed by both pathologists, and cytoplasmic and membranous staining were scored in a semi-quantitative fashion. Positivity of >5% of the tumor cells was necessary for scoring a case as positive. Staining intensity in positive cases was graded on a scale

of 1–3, where a staining intensity of 2 or 3 was considered strong. The mean value was recorded for each individual case as the average intensity of all 3 cores.

Results

HIG2 was positive in 143 of 155 cases (92%) of clear cell RCC with moderate and strong staining intensity in 79% of positive cases (mean value 2.14). Positive tumors exhibited coarse and fine granular cytoplasmic staining pattern with membranous accentuation (Figure 1). Papillary RCC were positive in 51 of 76 (67%) with moderate to strong staining in 83% of all positive cases (mean value 1.49). HIG2 expression in PRCC was also cytoplasmic and granular, but more focal and patchy than in CCRCC (Figure 2A). In 8 RCC with sarcomatoid dedifferentiation 6 were positive (75%) with either weak (4/6) or strong expression (2/6) (Figure 2B). In both clear cell and papillary RCC we found no significant correlation between HIG2 expression and tumor grade or size. In chromophobe RCC, the vast majority of cases (49/53, 92.5%) were negative with the HIG2 antibody. Only 4 cases exhibited any staining (2 weak and 2 moderate, mean value 0.11).

Oncocytomas were virtually negative for with the exception of 1 case (4.3%) exhibiting moderate reactivity (mean value 0.08) (Figure 3). Distribution of primary renal cortical tumors by HIG2 staining intensity is shown in Figure 4. We found a statistically significant difference of HIG2 expression between all studied RCC types ($p < 0.001$). Evaluation of HIG2 as a diagnostic test for CCRCC vs. ChRCC showed 92% sensitivity, 75% specificity, 97% positive predictive value, 80% negative predictive value and 92% accuracy.

Normal adjacent kidney tissues were negative in 50% cases (4/8) and weakly positive in renal tubules of the remaining 50% of cases (4/8) (Figure 5A). Fetal kidneys were focally weak positive in 1/3 cases (Figure 5B). HIG2 was completely negative in all 4 examined adrenals and 20 liver tissues. In 6 tonsils with reactive hyperplasia we detected only weak HIG2 expression in plasma cells.

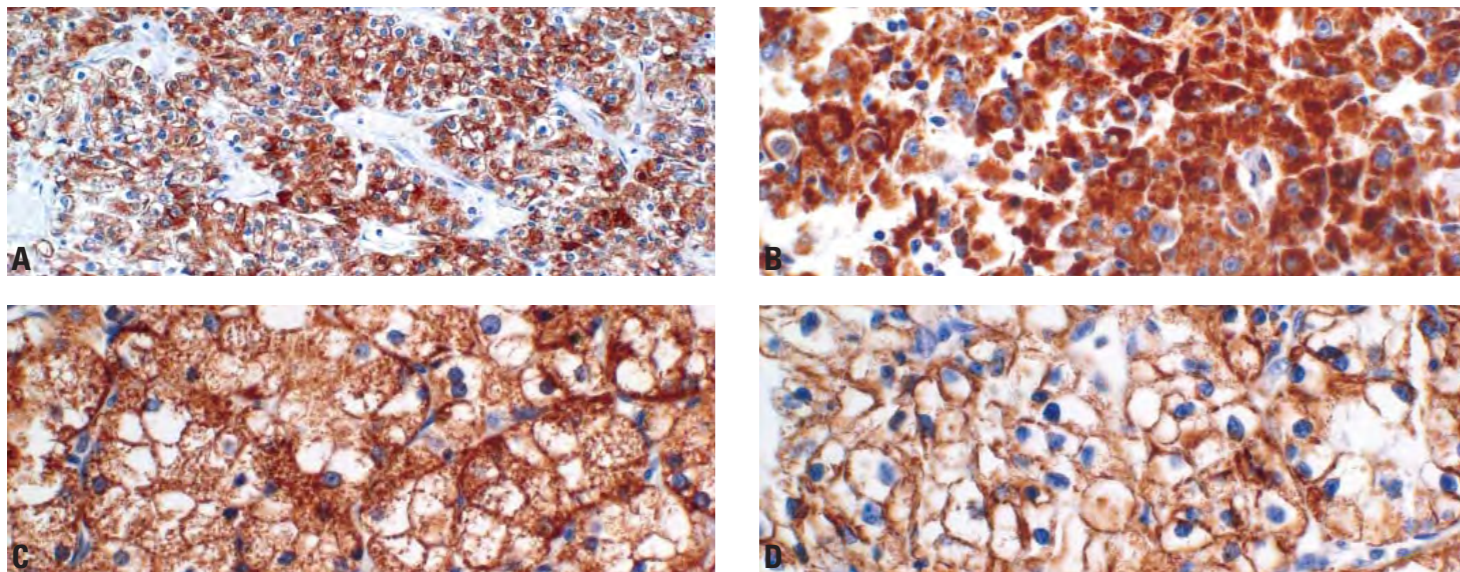


Figure 1. Expression of HIG2 in four representative cases of CCRCC: strong diffuse staining pattern (A), predominantly cytoplasmic HIG2 localization with coarse and fine granularity (B) mixed cytoplasmic and membranous HIG2 staining pattern (C), and predominantly membranous HIG2 localization (D). Original magnification x200 (A), original magnification x400 (B-D).

Discussion

HIG2 is strongly induced by hypoxia and glucose deprivation, and has been recognized as a very sensitive marker of unfavorable microenvironmental stresses characteristic to RCC among other tumors. An initial report showed similar stress responsiveness of HIG2 and VEGF suggesting that HIF-1 may play a role in HIG2 transcriptional regulation.⁵ However, a following study provided strong evidence that HIG2 overexpression in RCC is largely independent of either VHL or HIF-1 regulators.⁸ Moreover, further experiments showed that HIG2 induction resulted in cell growth enhancement and anti-apoptotic capability. By binding to an extracellular domain of frizzled homologue¹⁰, HIG2 protein boosted oncogenic Wnt signaling and its own transcription, suggesting its role as a hypoxia dependent autocrine growth factor.^{10, 11}

In this study of 308 primary renal tumors we found that the highest levels of HIG2 protein (clone HX34Y) expression was in conventional clear cell RCC (92%) followed by papillary RCC (67%). HIG2 staining pattern in CCRCC was predominantly diffuse cytoplasmic granular with some membranous accentuation, whereas PRCC exhibited more patchy cytoplasmic granular expression. In contrast, HIG2 was negative in the vast majority of ChRCC (92.5%) ($p < 0.001$). Benign oncocytomas were virtually non-reactive with HIG2 antibody with exception of a single case (4%). This differential expression of HIG2 in renal cortical tumors could be explained by the different mechanisms leading to hypoxia in different subtypes of RCC. CCRCC has a constitutively abnormal response to hypoxia by alteration in the VHL-HIF pathway^{7, 10}, whereas PRCC is naturally the least vascular in renal cortical tumors as has been previously shown.¹² In ChRCC, it is likely that this tumor, and to some degree benign oncocytoma, rarely develops hypoxic changes due to lack of oxygen stress reflecting its indolent course and slow growth rate in the majority of cases. Overall, the differential expression of HIG2 in RCC variants and its absence in ONC suggests its high sensitivity in detecting tumors with hypoxic stresses. Further comparison of HIG2 with other known hypoxia markers will help to understand its mechanism of function, and prognostic value in hypoxia-targeted therapies.

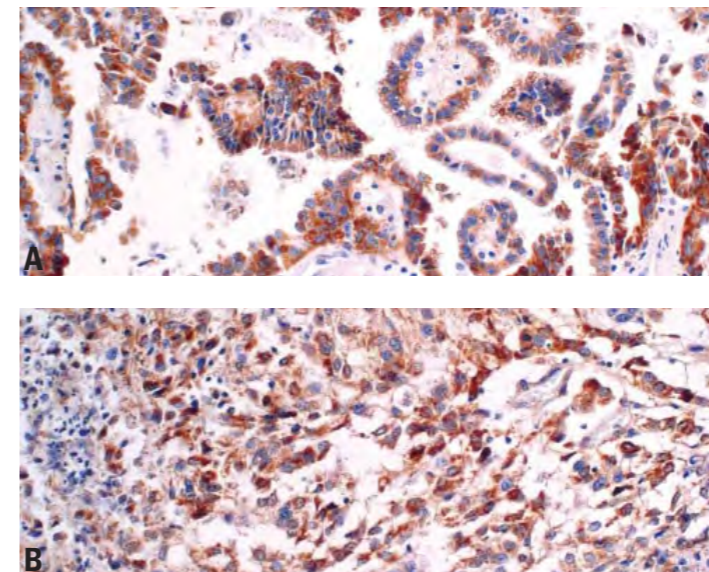


Figure 2. Patchy strong cytoplasmic expression of HIG2 in papillary RCC variant (A) and diffuse moderate in sarcomatoid dedifferentiated RCC (B). Original magnification x200.

Even though HIG2 expression is not unique to RCC, and was detected in ovarian clear cell carcinomas, cervical, and head and neck squamous cell carcinomas^{5, 7}, it may still have value in the differential diagnosis of CCRCC and ChRCC in the unusual situation of morphologic overlap, and especially in limited diagnostic material, such as needle biopsy. In our series we found 92% sensitivity and accuracy, and 97% PPV of HIG2 as IHC diagnostic test. HIG2 expression levels were retained in the majority of metastatic RCC (data not shown), making HIG2 by IHC a potentially useful test for diagnosing of metastasis with unknown primary. Interestingly, Togashi et al¹⁰ in their ELISA experiments identified increased HIG2 protein secretion into the plasma of RCC patients at both early stage of tumor development and in metastatic disease.

Forty one normal tissues examined in our study showed preferential expression of HIG2 in renal tubules in 1 out of 3 fetal kidney and 4 of 8 adult kidneys adjacent to RCC. Interestingly, tubular expression of HIG2 was only observed in cases with interstitial fibrosis indirectly proving high HIG2 sensitivity to hypoxic conditions.

The HIG2 gene encodes a 63 amino acid trans-membrane protein of 7kD molecular weight which in co-localization experiments was found within endoplasmic reticulum and Golgi apparatus, but not in mitochondria, lysosomes, endosomes or lipid droplets.¹¹ In our experience mouse monoclonal HIG2 antibody (clone HX34Y), developed by Leica Biosystems research team, is user friendly, gives reproducible, clean and crisp granular staining of cytoplasm associated with some membranous accentuation especially in CCRCC. We did not appreciate any stromal background with this HIG2 antibody, thus making IHC scoring and interpretation straightforward.

In summary, our data strongly indicate that HIG2 is a promising surrogate marker of hypoxia in both CCRCC and PRCC, but further comparison with well established hypoxia markers and prognostic studies is warranted.

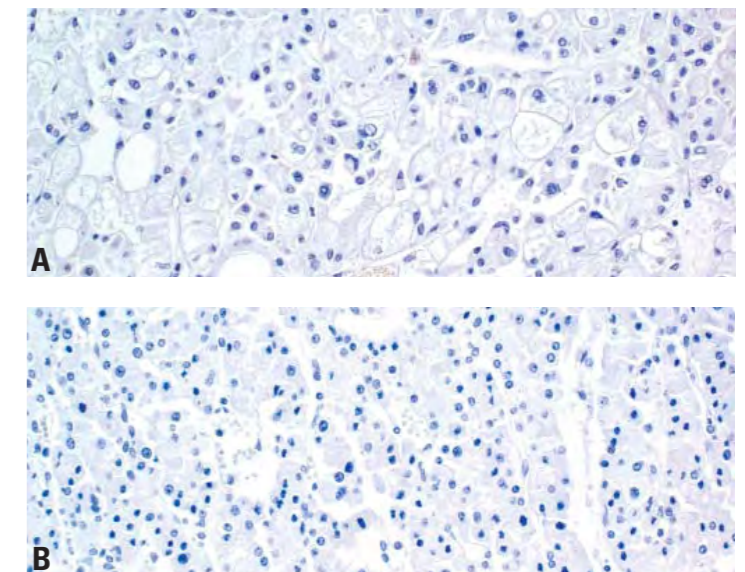


Figure 3. Complete lack of HIG2 expression in representative cases of ChRCC (A) and ONC (B). Original magnification x200.

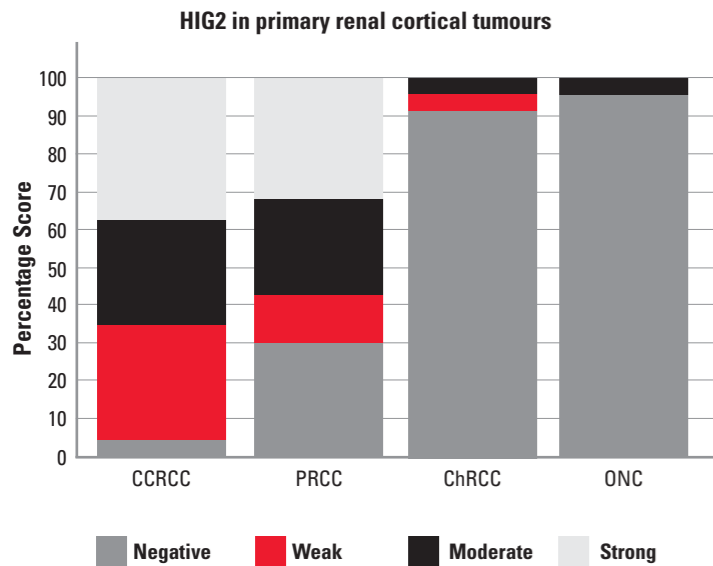


Figure 4. Distribution HIG2 by staining intensity in primary cortical tumours: note highest levels of HIG2 expression in CCRCC followed by PRCC, and dramatic decline in HIG2 presence in ChRCC and ONC.

Conclusion

The antibody against HIG2 protein (clone HX34Y) showed crisp cytoplasmic granular staining pattern which could be admixed with membranous labeling, but was free of any non-specific background binding to stromal or inflammatory cells. HIG2 expression was present in the majority of CCRCC (92%) and PRCC (67%), the two most common subtypes of RCC, but largely negative in ChRCC and ONC. In normal kidneys HIG2 expression was noted only in cases with stromal fibrosis. Our findings suggest that HIG2 is a sensitive hypoxia marker and has a great potential as a diagnostic and prognostic marker in RCC.

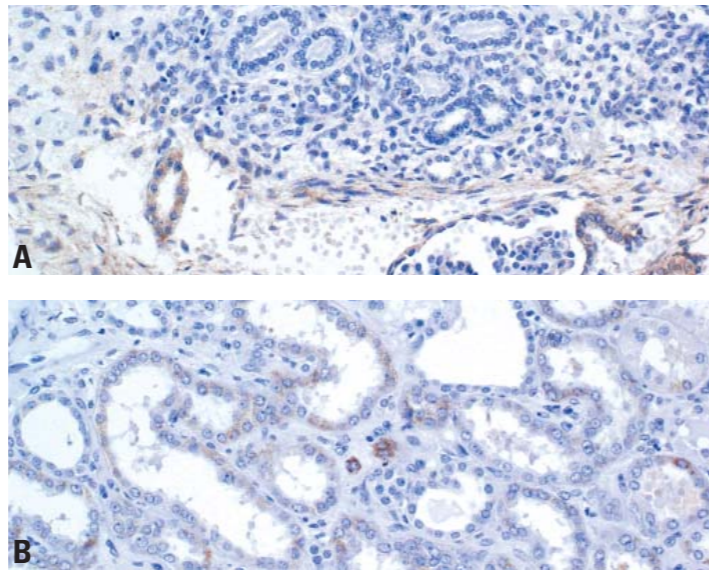


Figure 5. HIG2 expression in normal kidneys: fetal kidney with cytoplasmic positivity in some tubules (A), adjacent to RCC adult kidney with HIG2 expression in tubules surrounded by stroma with mild interstitial fibrosis (B). Original magnification x200.

References

- Eble JN TK, Pisani P. Pathology and genetics: tumours of the urinary system and male genital organs. 1 ed. Lyon: IARC Press; 2004.
- Hock LM, Lynch J, Balaji KC. Increasing incidence of all stages of kidney cancer in the last 2 decades in the United States: an analysis of surveillance, epidemiology and end results program data. *J Urol* 2002;167(1):57-60.
- Smaldone MC, Maranchie JK. Clinical implications of hypoxia inducible factor in renal cell carcinoma. *Urol Oncol* 2009;27(3):238-45.
- Bukowski RM. Targeted therapy for cytokine-refractory metastatic renal cell carcinoma, and treatment in the community. *Oncology (Williston Park)* 2006;20(6 Suppl 5):25-8.
- Denko N, Schindler C, Koong A, et al. Epigenetic regulation of gene expression in cervical cancer cells by the tumor microenvironment. *Clin Cancer Res* 2000;6(2):480-7.
- Togashi A, Katagiri T, Ashida S, et al. Hypoxia-inducible protein 2 (HIG2), a novel diagnostic marker for renal cell carcinoma and potential target for molecular therapy. *Cancer Res* 2005;65(11):4817-26.
- Kaelin WG, Jr. Treatment of kidney cancer: insights provided by the VHL tumor-suppressor protein. *Cancer* 2009;115 (10 Suppl):2262-72.
- Le QT, Kong C, Lavori PW, et al. Expression and prognostic significance of a panel of tissue hypoxia markers in head-and-neck squamous cell carcinomas. *Int J Radiat Oncol Biol Phys* 2007;69(1):167-75.
- Stroka DM, Burkhardt T, Desbaillets I, et al. HIF-1 is expressed in normoxic tissue and displays an organ-specific regulation under systemic hypoxia. *Faseb J* 2001;15(13):2445-53.
- Klatte T, Seligson DB, Riggs SB, et al. Hypoxia-inducible factor 1 alpha in clear cell renal cell carcinoma. *Clin Cancer Res* 2007;13(24):7388-93.
- Kenny PA, Enver T, Ashworth A. Receptor and secreted targets of Wnt-1/beta-catenin signalling in mouse mammary epithelial cells. *BMC Cancer* 2005;5:3.
- Al-Ahmadie HA, Olgac S, Gregor PD, et al. Expression of prostate-specific membrane antigen in renal cortical tumours. *Mod Pathol* 2008;21(6):727-32.

Prospective Evaluation of New CD19, CD30 and CD7 Antibodies for Fixed Tissue Immunohistochemistry

Wilkins BS^{1,2}, Menon G², Cowell S³, Hall M³, Piggott NH³, Scorer P³, Tristram C³, McIntosh G³

- Northern Institute for Cancer Research, UK
- Newcastle University, Newcastle upon Tyne Hospitals NHS Foundation Trust, UK
- Leica Biosystems, Newcastle upon Tyne, UK

Introduction

The North East Haematopathology Diagnostic Service, based at the Royal Victoria Infirmary in Newcastle upon Tyne, provides a regional service for expert assessment of lymphoproliferative and myeloproliferative disorders for a regional network of 14 NHS hospitals in the North East and Cumbria.

Provision of an extensive repertoire of immunohistochemistry is essential for this service, and methods employed must be suitable for successful use with material fixed and processed according to protocols that vary considerably between submitting hospitals.

Access to material representing a wide range of diagnoses, in a great variety of tissues, diversely processed for histology has provided us with an excellent opportunity to undertake a systematic, prospective evaluation of three new monoclonal antibodies, NCL-L-CD7-580, NCL-L-CD19-163 and NCL-L-CD30-591 (Novocastra™, Leica Biosystems, Newcastle, UK) alongside our standard antibody panels in regular use.

Methods

For a three month period, a new anti-CD19 monoclonal antibody (clone BT51E) was added to our standard basic lymphoid cell immunostaining panel (CD20, CD79a, CD2, CD3 and Ki67). A new anti-CD30 clone (JCM182) was added in to our "Hodgkin panel" which currently employs the CD30 antibody clone BerH2 plus monoclonal antibodies reactive with CD15, CD45, EBV-LMP1 and EMA. A new anti-CD7 clone (LP15) was added to our extended panel for investigation of putative T cell lymphomas (CD4, CD5, CD7 (CD7-272), CD8, CD43, CD45RO and CD246/ALK1).

Sections stained with the novel antibodies were scored semi-quantitatively by two assessors (BW, GM) at the time of histological evaluation of cases and scores also assigned on the same basis to sections stained with our regular antibodies.

Ideal staining scored 3, with scores of 2 and 1 being assigned to cases with mildly or markedly reduced intensity of staining. A score of 0 was given if staining failed completely. Scores were then analysed as a percentage of the maximum score possible for the number of cases assessed. During the 3-month period, 100 cases were accrued that required staining with at least one of the immunohistochemical panels.

Results

This strategy provided a very thorough assessment of CD19 in comparison with our current standard B cell markers and also gave useful insight into the comparative performance of the new CD30 clone.

However, only a small number of putative T cell lymphomas were evaluated with the extended T cell phenotyping panel during the study period, so that information for this reagent is only anecdotal.

Scores were analysed as a percentage of the maximum score possible for the number of cases assessed and the results are shown in Figure 1.

For CD19, sufficient cases were available to analyse the results according to source for the six largest hospitals in the network. Bone marrow trephine specimens were omitted from this sub-analysis, since decalcification methods are known to vary between these hospitals. Scores were also analysed according to the tissue type and diagnosis, to evaluate whether these factors influenced the quality of staining. The CD19 antibody gave equivalent strong staining to that for CD20 or CD79a in many cases but was rather more variable overall (Figure 1).

This was not significantly influenced by variations in fixation and processing that exists between the different hospitals in our network. Variation apparently linked to the underlying diagnosis in fact largely reflected differences in tissue type, with decalcification of bone marrow trephine specimens (using either formic acid or chelation in different hospitals) having an adverse effect on staining quality (Figure 2A-C). Reduction in staining quality found with spleens is likely to reflect the slow and often suboptimal fixation achieved for splenectomy specimens; although it is unclear why there should be an adverse effect for tonsils.

The numerical scores do not do full justice to the results obtained, however, the staining for CD19 was crisp and easy to interpret in the many good preparations, staining a wider spectrum of B lineage cells than CD20 and subjectively easier to assess in many cases than CD79a.

One major advantage of the availability of this new CD19 antibody is that it creates greater comparability between flow cytometric immunostaining of fresh cells and fixed tissue immunohistochemistry.¹ It can also provide an additional B cell surface marker for use in complex lymphoid proliferations and those with down-regulated CD20 expression following anti-CD20 immunotherapy.²

For CD30, the new clone, JCM182, out-performed the current gold-standard BerH2 clone in almost all of the 25 cases studied (Figure 3, 4A & B). The interpretation was generally unequivocal although non-specialists should be aware that a population of medium-sized to large activated perifollicular cells, predominantly intra- and peri-follicular in distribution, express CD30³ and these are more clearly apparent in sections immunostained with the new antibody, clone JCM182.

For CD7, our study included too few examples for anything more than anecdotal comment. However, the new antibody performed well (Figure 5A & B), giving an overall score of 93% in the 7 cases examined, in comparison with 73% scored by our current antibody. A major improvement in sections stained for CD7 with the new clone is the absence of the strong nucleolar staining that occurs commonly with clone CD7-272.

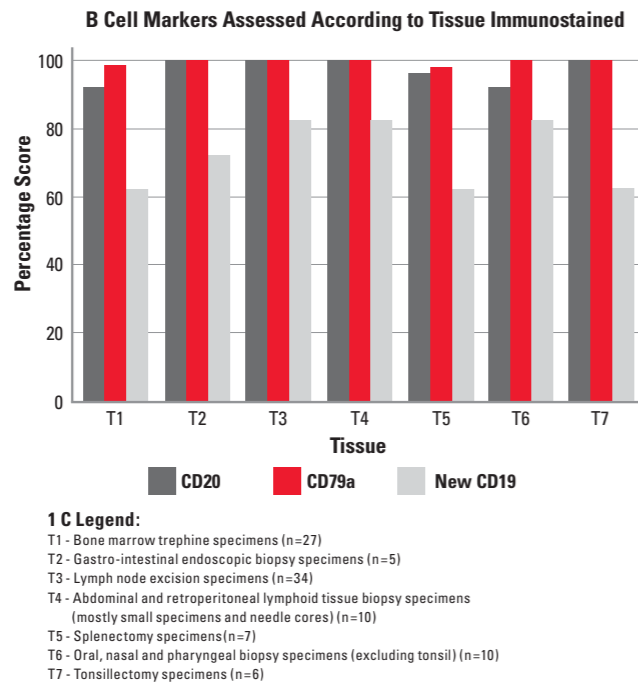
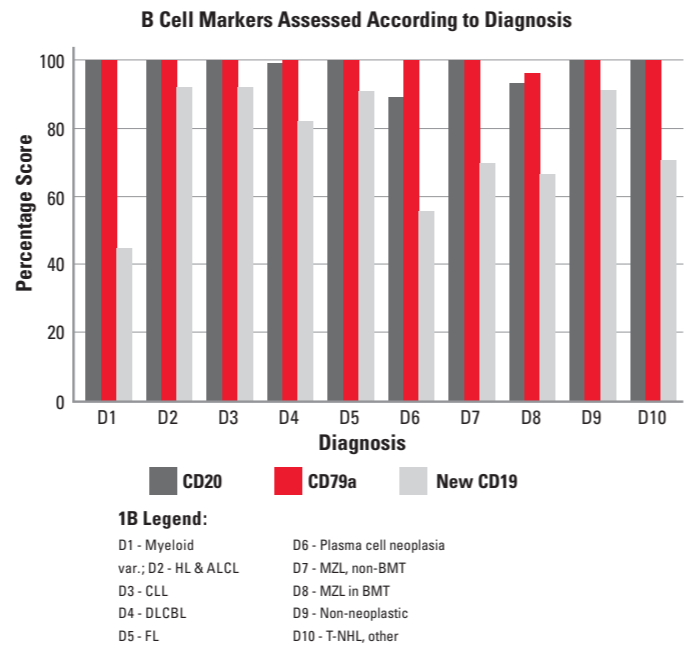
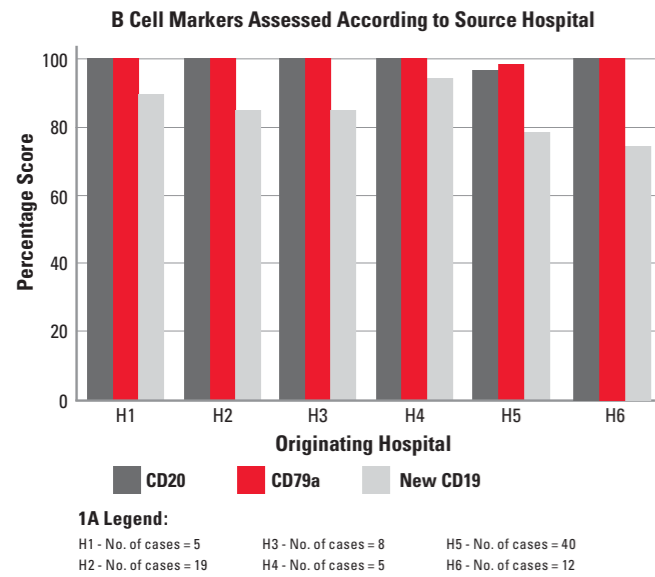


Figure 1A,1B & 1C. Performance of C19 (clone BT51E) in comparison with CD20 and CD 79A.

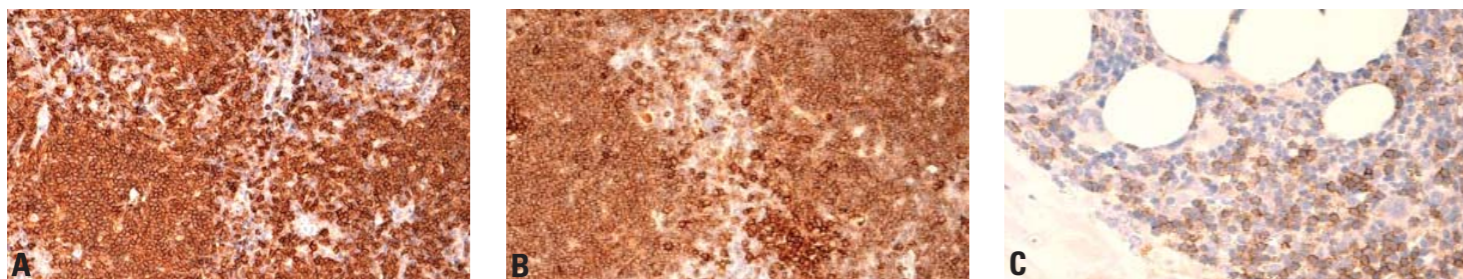


Figure 2A, 2B & 2C. Performance of CD19 BT51E on lymph nodes involved by follicular lymphoma. 2C is a bone marrow trephine specimen infiltrated by splenic marginal zone B cell lymphoma. Original magnification x200. Paraffin sections.

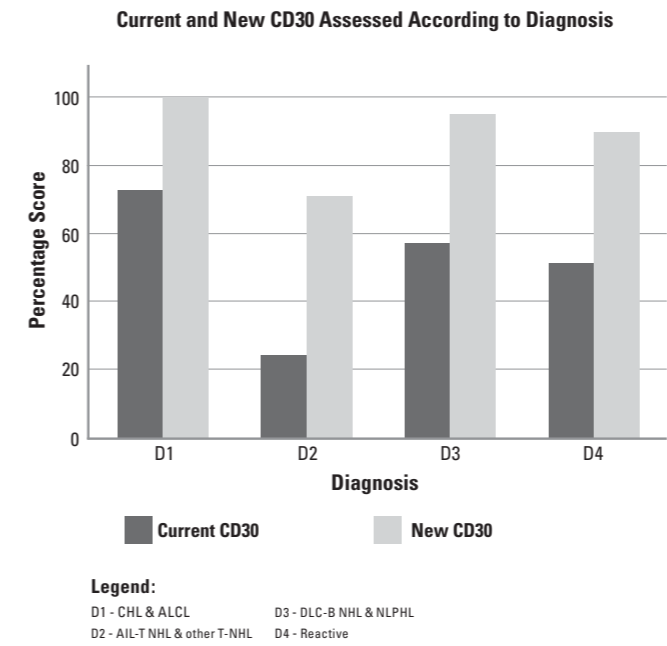


Figure 3. CD3 – Comparison between the CD30 clones BerH2 and JCM182

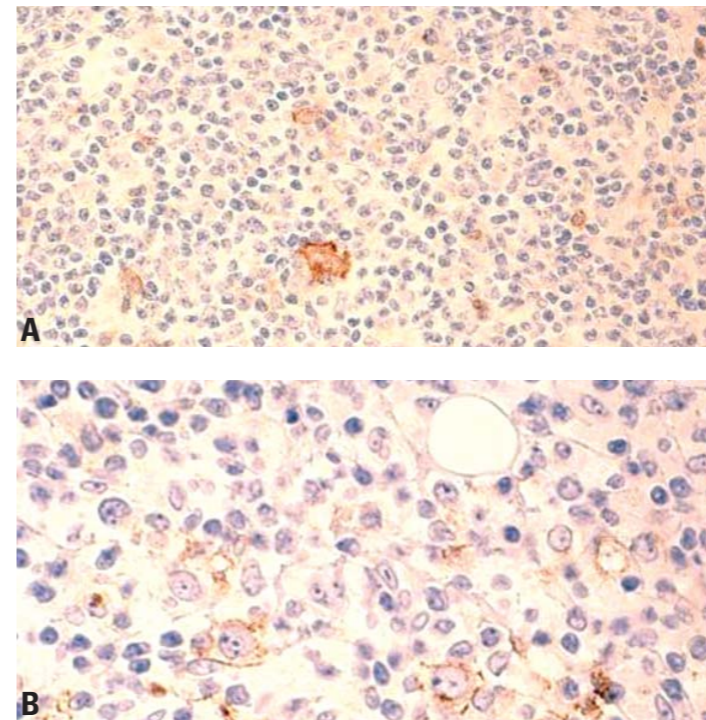


Figure 4. CD30 – Typical images of JCM182(A) (original magnification x200) & BerH2 (B) (original magnification x400). Reactive lymph node. Paraffin sections.

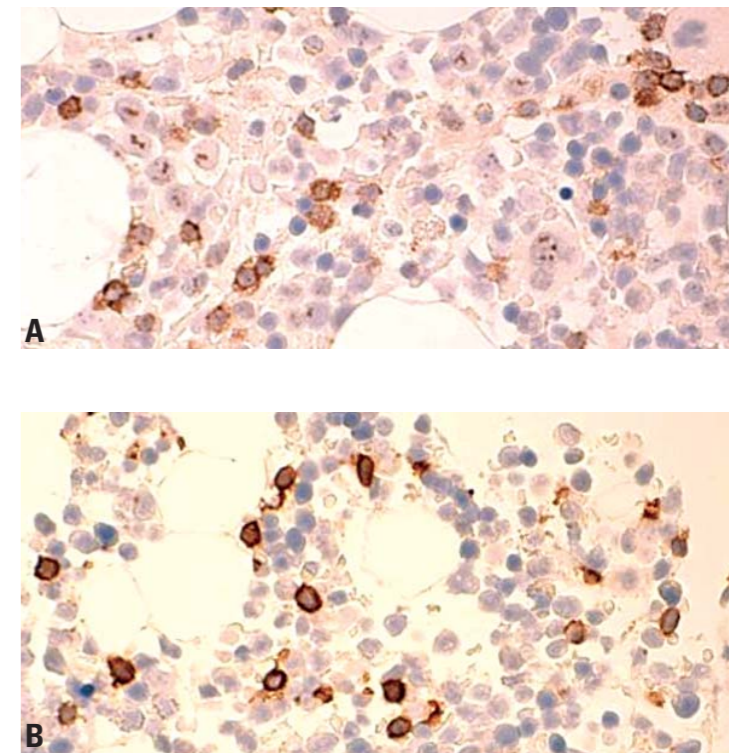


Figure 5. CD7 – Performance of clone CD7-272 (A) and clone LP15 (B) on normal bone marrow. Original magnification x400. Paraffin sections.

Conclusion

Prospective testing of three novel antibodies for immunohistochemistry alongside routine panels in a busy diagnostic laboratory provided a simple and cost-effective strategy to evaluate the performance of the CD19 reagent, because of the frequency and range of material with which it could be tested.

This kind of small scale study is difficult to justify and fund independently as “research” in the current UK research climate but is essential for appropriate validation of novel reagents as they are developed for potential diagnostic use. Our strategy was less successful for the CD30 and, in particular, CD7 reagents because we made less frequent use of immunostaining panels requiring these antibodies than we anticipated in the 3-month study period.

Retrospective analysis of a selected cohort of cases would be the method of choice for such antibodies not included in an immunostaining panel applied to a high proportion of routine cases.

References

- Dunphy CH (2004). Applications of flow cytometry and immunohistochemistry to diagnostic hematopathology. Archives of Pathology and Laboratory Medicine: 128 (9), 1004-1022.
- Foran JM, Norton AJ, Micallef INM, et al (2001). Loss of CD20 expression following treatment with rituximab (chimaeric monoclonal anti-CD20): a retrospective cohort analysis. British Journal of Haematology: 114(4), 881-883.
- Segal GH, Kjeldsberg CR, Smith GP, et al (1994). CD30 antigen expression in florid immunoblastic proliferations. A clinicopathologic study of 14 cases. American Journal of Clinical Pathology: 102(3), 292-298.

3D Histopathology of the Liver Using Dual Chromogen Histochemistry

Ismail A¹, Gray S², Jackson P², Shires M¹, Crellin DM¹, Magee D³, Quirke P¹, Treanor D¹

1. Pathology and Tumour Biology, L IMM, University of Leeds, UK
2. Histopathology Department, Leeds Teaching Hospital's Trust, UK
3. School of Computing, University of Leeds, UK

Abstract

Three dimensional reconstruction of liver tissue is beneficial as it can improve understanding of the normal architecture of the vascular and biliary system; additionally, awareness of how these systems are affected by various pathological processes may help to inform future treatment choices.¹

We aimed to reconstruct in three-dimension the vascular and biliary system of the liver. By using the Bond™ system we were able to carry out double immunohistochemical staining for the primary antibodies CD34 and CK19, producing consistent results in a reduced amount of time. This was useful, as the dual chromogen staining made it easier to highlight the blood vessels and bile ducts of the liver in the same sections, giving more accurate three dimensional models.

Introduction

Immunohistochemical staining is useful diagnostically, as it can highlight ways in which pathological processes manifest themselves in various tissues.² Visualising two antigens in the same tissue is essential in a variety of settings including when trying to identify combinations of surface markers and mapping receptor and ligand distribution across a cell.³

Using the alkaline phosphatase and peroxidase protocols together has made it possible to view two different cellular markers in the tissue section, revealing two colours: red (for the alkaline phosphatase) and brown (for the peroxidase). The colours produced by the antibody-antigen reactions have no significant bearing on the amount of reaction product present. Colour deconvolution can be useful in segmentation of immunostained structures.⁴ It allows endothelial cells to be correctly identified through defining the stain colour vectors. Different colours are used to segment different types of tissues or cellular components, which can prove useful from a pathological or histological perspective.

The aim of this study was to reconstruct the vascular and biliary system of normal human liver (central and peripheral specimens) in three-dimension, using the Bond-max™ immunostainer to detect CD34 and CK19 antigens. The Bond-max immunostaining system was used to demonstrate an enhanced quality and quantity of stained slides produced in a given time and also to demonstrate how automated immunostainers can be implemented within the research environment. The images produced would then be used to produce computerised three-dimensional models of different aspects of the liver tissue (See Figure 1).

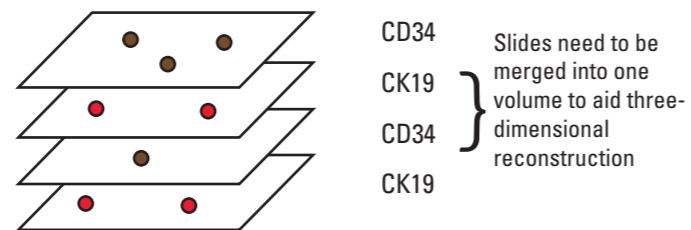


Figure 1A. Single vs Dual Chromogen Staining (brown = CD34, red = CK19). Fig 1a demonstrates single chromogen staining for CD34 and CK19. Because each slide only contains one stain, both sets of stains would need to be combined (merged into one volume) to allow effective reconstruction of the tissue components.

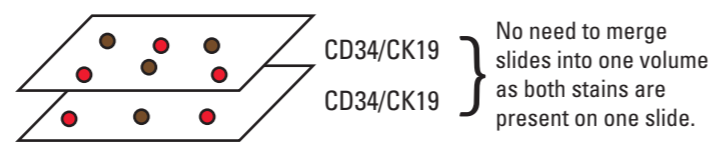


Figure 1B. Demonstrates dual chromogen staining whereby both stains are present on one slide. It is easy to see that this process uses less glass slides and the fact that each slide contains more detailed information means that reconstruction of both the epithelium and endothelium can be carried out simultaneously rather than having to switch between CD34 and CK19 slides in the single chromogen technique.

Materials and Methods

Tissue Specimens

Formalin-fixed paraffin-embedded (FFPE) normal human (central and peripheral) liver specimens were obtained from the authors' institution.

Double Immunohistochemical Staining

Staining was carried out by using ready-to-use primary antibodies CD34 (QEnd/10) and CK19. Protocol F, with the haematoxylin step omitted and Protocol G were used, with antigen retrieval set as ER2 for 20 minutes. It was possible to combine both of these protocols, therefore only one set of adhesive labels needed to be printed.

The adhesive labels were printed and applied to each slide, which had been stored in the fridge overnight; these were then loaded into the racks which had a maximum capacity of 10 slides. The Bond Universal Covertiles were then placed upon each slide and then the racks were loaded into the immunostainer; this had a maximum capacity of thirty slides (three racks at a time). Washing between the reagents involved the use of the Bond Wash Solution, which required a 1 in 10 dilution prior to use.

The sections being stained were from FFPE human liver blocks. The tissue was fixed in 10% neutral buffered formalin (Sigma – Poole, Dorset) for a minimum of 48 hours. The tissue was processed using a Leica ASP200 (Leica Microsystems, Milton Keynes, UK) along the schedule listed below (Table 1):

Reagent	Time – hours
70% ethanol	1
80% ethanol	1
90% ethanol	2
95% ethanol	2
100% ethanol	3x3
Xylene	1
Xylene	3
Xylene	6
Wax	1
Wax	3
Wax	6

Table 1. Tumor Processing Schedule.

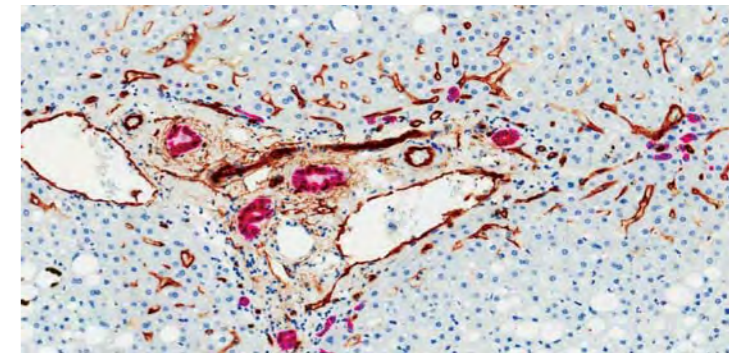


Figure 2. Dual Chromogen Staining of normal human liver. This figure shows dual chromogen staining for CD34 and CK19, for a normal human liver. The brown colour represents the endothelial tissue of portal vessels, whereas the red stain represents the epithelial tissue of bile ducts and ductules.

The tissue was embedded using a Leica EG1150H Embedding Station in Cell Wax plus (Cell Path - Newton, Powys). Serial sections were cut at 4 µm on a Leica RM2255 microtome. 5 serial sections were cut at a time, followed by a 40 µm gap through the entire tissue block.

Two polymer detection systems from Leica Microsystems were used. The Bond Polymer Refine (DS9800), a peroxidase based detection reagent and the Bond Polymer AP Red (DS9305), an alkaline phosphatase detection reagent were used. The slides were counterstained with haematoxylin, which is included within the Bond Polymer AP Red detection system.

Antibodies

The primary antibodies used for this study included: CD34 (clone QEnd/10, PA0212), a mouse anti-human monoclonal antibody and CK19 (clone b170, PA0799), also a mouse anti-human monoclonal antibody. These antibodies were in a ready-to-use mixture.

The immunohistochemical slides produced were scanned in sequence giving virtual images of the stained sections. A programme was used to generate volumes which contained all the images of all the slides sectioned and stained in each block. Following this, the tissue could be reconstructed to generate three-dimensional models of the vascular and biliary system in the normal liver.

Results

The results obtained showed that by using dual chromogen staining, it became easier to reconstruct the tissue in three-dimensions; this is because the epithelium and endothelium were easily visible on one slide and could be reconstructed in one three-dimensional reconstruction rather than merging two separate reconstructions which takes much more time. With the Bond-max immunostainer, staining was consistent and avoided unspecific staining of background areas. Examples of the dual chromogen immunohistochemical staining for CD34 and CK19 in a normal human liver are shown (see Figure 2 and 3).

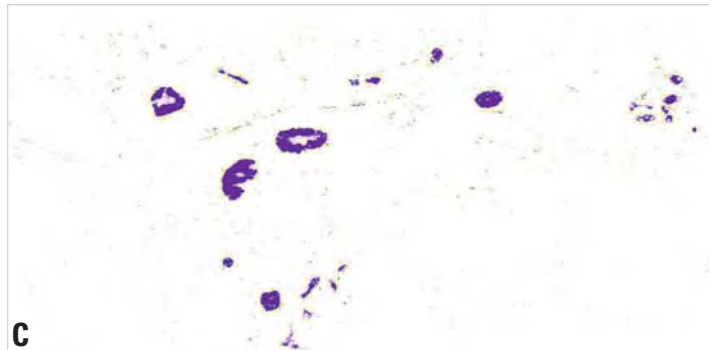
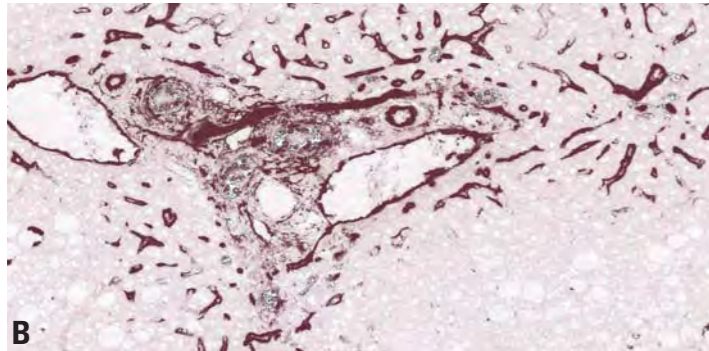
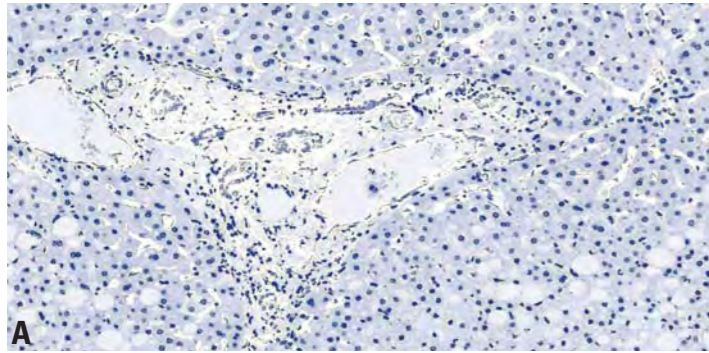


Figure 3. Colour Deconvolution of Figure 2B. This process allows automatic separation of the haematoxylin and both chromogens, generating 3 separate images showing (from top to bottom) nuclei (haematoxylin channel), biliary epithelial cells (CK19-DAB channel) and vessels (CD34-Alk phos channel).

Discussion

This study demonstrated that by carrying out dual chromogen staining, it becomes much easier to reconstruct the tissue in three-dimension as more information is contained on one slide. This avoids having to switch between slides to look at different immunohistochemical stained volumes.

The use of the automated immunostainer provided consistent staining between different batches of slides and also reduced the degree of background staining. Using the manual protocol is time consuming and can result in tissue damage due to pressure cooking and inconsistent results.

This can make it difficult to interpret the results or carry out clinically relevant analysis. This in turn creates problems for laboratories routinely using these techniques for diagnostic purposes.

The benefit of using dual chromogen staining is the ability to combine two completely different detection systems to produce the two-labelled products, which can be clearly distinguished from one another.

Tissue damage (which is often encountered when using pressure cooker antigen retrieval) was reduced due to on-board antigen retrieval.

Conclusion

This study shows dual chromogen staining can significantly improve and ease three-dimensional reconstruction of liver tissue. The presence of two stains on one slide not only provides benefit in terms of using less resources but it also allows simultaneous reconstruction to be done on the different stained components. 50% fewer glass slides were used, which in turn reduced the amount of technical time spent on doing the three-dimensional reconstructions.

Ms Ismail acknowledges the support of Heart Research UK in providing a LURE scholarship.

References

- Hano H, Takasaki S. Three-dimensional observations on the alterations of lobular architecture in chronic hepatitis with special reference to its angioarchitecture for a better understanding of the formal pathogenesis of liver cirrhosis. *Virchows Arch.* 2003;443:655-63.
- Glass G, Papin JA, Mandell JW. SIMPLE: A Sequential Immunoperoxidase Labeling and Erasing Method. *J. Histochem. and Cytochem.* 2009;57(10):899-905.
- Eichmiiller S, Stevenson PA, Paus R. A new method for double immunolabelling with primary antibodies from identical species. *J. Immunol. Methods* 1996;190:255-65.
- Ruifrok AC, Johnston DA. Quantification of histochemical staining by color deconvolution. *Anal Quant Cytol Histol* 23: 291-299, 2001.

Immunohistochemical Analysis of Carbonic Anhydrase IX (CA IX) in Renal Cortical Tumors

Illei PB, MD

Department of Pathology, Johns Hopkins University, USA

Abstract

A subset of renal cortical tumors cannot be accurately classified based on their morphologic features owing to partial overlap in their histologic appearance. Since the prognosis is different and clear cell carcinomas may be treated by the different therapeutic regimens there is a need for accurate classification.

A number of markers have been tested to assist in this task, but even when several markers are used a significant number of tumors remain unclassifiable. Carbonic anhydrase IX (CA IX) plays an important role in maintaining the pH of several tumor types. It is a stable cell surface protein that is amenable for detection by immunohistochemistry. CA IX has been found to be expressed in clear cell renal cell carcinoma (RCC) and type 1 papillary renal cell carcinoma. In this study, we have investigated the expression pattern of CA IX in 44 papillary RCC, 42 clear cell RCC, 37 chromophobe RCC and 28 oncocytomas.

The majority (95%) of clear cell RCC were positive, whereas only two cases (5%) of papillary RCC showed focal positivity. All chromophobe RCC and oncocytoma were negative. Immunohistochemistry for CA IX can be easily performed and positive staining in the absence of papillary features strongly suggest clear cell RCC.

Introduction

Renal cortical tumors can be classified according to their histologic appearance and/or genetic abnormalities.^{1,2} A minority (5%) of tumors cannot be typed owing to overlap in their morphologic features and to a lesser degree also in their genetic alterations.^{2,3} Accurate classification is important since different tumors have different prognosis and clear cell carcinomas may be treated differently.

Furthermore, the increased use of core biopsy to diagnose small tumors that are ablated at the time the biopsy is performed and tumors of patients who are poor surgical candidates increases the need for accurate typing on limited amounts of tissue. Commonly used antibodies including cytokeratin AE1/AE3, Pax-2, PAX-8, CK7, CK20, RCC, CD10, and vimentin can be helpful but do not provide definitive answer in a subset of cases.⁴⁻⁷

Recently, a new antibody became available for studying carbonic anhydrase IX (CA IX) expression in formalin fixed paraffin embedded tissue sections. Carbonic anhydrases are widely expressed in living organisms including in mammalian cells with 15 recognized isoenzymes.⁸⁻¹¹ They catalyze reversible hydration of carbon dioxide ($H_2O + CO_2 = H^+ + HCO_3^-$) that results in a net extrusion of H^+ and an increase in intracellular pH. The maintenance of pH during hypoxia is a key protective mechanism to prevent hypoxia induced cell death. Hypoxia upregulates the activity of a number of genes through hypoxia inducible factor-1 α (HIF-1 α) including two carbonic anhydrases (CA IX and CA XII).⁸⁻¹¹ CA IX is a 54/58 KDa transmembrane glycoprotein that has a cell surface enzyme activity and can be detected in normal gastrointestinal mucosa and a number of different tumors.

In the kidney, CA IX overexpression has been described in clear cell renal cell carcinoma and in type 1 papillary renal cell carcinoma but not in normal renal tissue.¹⁰⁻¹¹ In this study, our aim was to investigate the expression patterns of CA IX in the most common types of renal cortical neoplasms and to determine whether CA IX expression can be helpful for differentiating these tumor types.

Materials and Methods

Five micron sections of previously constructed tissue microarrays (TMA) of 44 papillary RCC, 42 clear cell renal cell RCC, 37 chromophobe RCC and 28 oncocytomas were subjected to immunohistochemistry using a mouse monoclonal antibody for CA IX (Leica Biosystems, Newcastle, UK) on a Leica Bond™ automated stainer (Leica Microsystems, Bannockburn, IL). The TMA also included samples of benign brain, pancreas, kidney, thyroid, testis, lung, smooth muscle, liver, tonsil, thymus, skin, small intestine, ovary and fibroconnective tissue.

The staining was evaluated according to criteria listed in Table 1. The scores of both intensity and extent were added and a stain was considered positive with a combined score of greater than 2.

Score	0	1	2	3
Intensity	No staining	weak	moderate	strong
Extent	No staining	<25%	25-50%	>50%

Table 1. Scoring criteria for intensity and extent of staining of tumor cells.

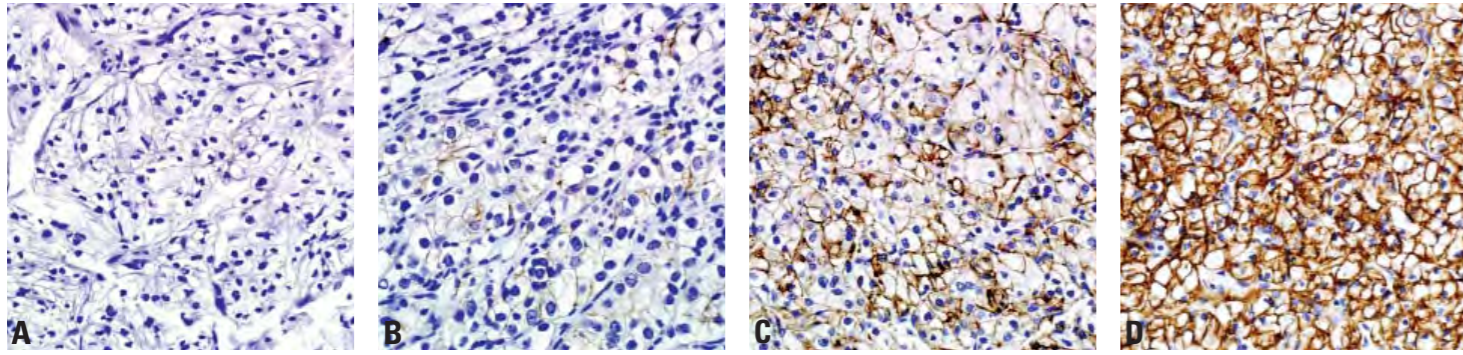


Figure 1. CA IX immunohistochemistry of Clear cell renal cell carcinoma. A. Negative tumor (no staining); B. Focal weak staining (score 2); C. Diffuse moderate staining (score 5); D. diffuse strong staining (score 6).

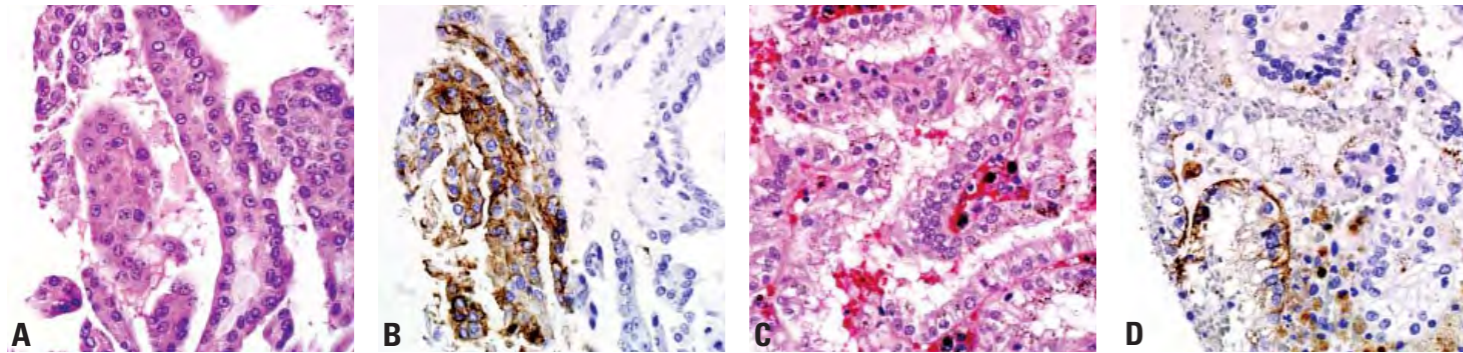


Figure 2. CA IX immunohistochemistry of the positive papillary cell renal cell carcinoma. A. Hematoxylin eosin stained section of tumor #1. B. Focal strong CA IX staining (score 4) of tumor #1. C. Hematoxylin eosin stained section of tumor #2. D. Focal moderate CA IX staining (score 3) of tumor #2.

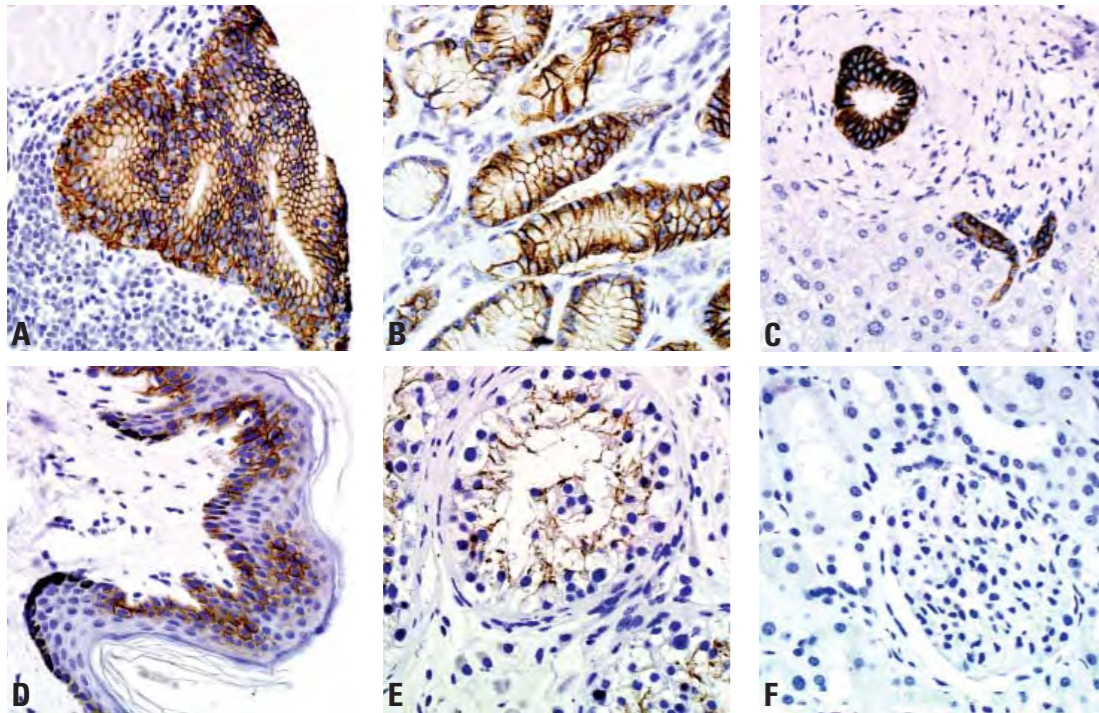


Figure 3. CA IX immunohistochemistry of benign tissues. Strong membranous staining is observed in gallbladder (A) and gastric (B) mucosa, in intrahepatic bile duct epithelium (C). Weak-moderate staining of epidermis (D) and Sertoli cells in the testis (E). Negative normal renal parenchyma (F).

Results

The results are summarized in Table 2. The majority (95%) of clear cell RCC were positive for CA IX with most cases showing moderate (2+) to strong (3+) staining in over 50% of the tumor cells (Figure 1).

	CAIX Positive
Clear Cell RCC	39/41 (95%)
Papillary RCC	2/44 (5%)
Chromophobe RCC	0/37 (0%)
Oncocytoma	0/28 (0%)

Table 2. Results of CA IX immunostaining of clear cell renal cell carcinoma (RCC), Papillary RCC (PRCC), chromophobe renal cell carcinoma (ChRCC) and oncocytoma.

The papillary RCC TMA contained both type 1 and type 2 tumors. The two positive cases (5%) were both type 1 and showed moderate to strong membranous staining in less than 25 % of the tumor cells (Figure 2). All chromophobe RCC and oncocytomas were negative for CA IX.

Of the benign tissues strong membranous staining was noted in gastric, small bowel, and gallbladder mucosa, and in intrahepatic bile duct epithelium (Figure 3).

Diffuse weak to moderate staining was noted in Sertoli cells and focal weak to moderate staining was seen in the epidermis (Figure 3). All other benign tissues including kidney were negative (Figure 3).

Discussion

Since a subset of renal cortical tumors cannot be classified even when using current ancillary techniques there is a need for additional markers that can assist in this effort. CA IX is present in a number of tumors and in some benign tissues and is one of the most uniformly induced genes in hypoxia. Since CA IX is a stable cell surface protein it is a good target for immunohistochemical detection. Under normal physiologic conditions CA IX expression is largely limited to the GI tract mucosa. CA IX is also expressed in a number of tumors which include some of the most aggressive types of cancer. Some authors have recommended using CA IX expression by immunohistochemistry as a marker of hypoxia¹², moreover CA IX has also been investigated as target for therapy.¹³⁻¹⁶

In our study, we found CA IX expression in the large majority of clear cell RCC, but not in chromophobe RCC or oncocytomas. There were only two papillary renal RCC (both type 1) that were positive and both cases showed less extensive staining of the tumor. As expected normal renal cortex and medulla were negative and strong staining was noted in mucosa from the upper gastrointestinal tract and intrahepatic bile duct epithelium.

Conclusions

Immunohistochemistry for CA IX can be easily performed on paraffin-embedded formalin-fixed tissue. CA IX immunostains can be used to differentiate clear cell RCC from chromophobe RCC and oncocytoma. Focal staining can be seen in a small subset of type 1 papillary RCC where careful examination of the histologic features should be performed and the use of additional markers should be considered. Furthermore, since CA IX plays an important role in maintaining the tumor cell homeostasis and in preventing cell death induced by hypoxia it is a potential candidate for targeted therapy.

References

1. Pathology and genetics: Tumors of the urinary system and male genital organs. World Health Organization classification of tumors. IARC Press 2006.
2. Kovacs G, Akhtar M, Beckwith BJ, et al. The Heidelberg classification of renal cell tumours. *J Pathol* 1997;183:131-133.
3. Barocas DA, Rojan SM, Kao J et al. Diagnosis of renal tumors on needle biopsy specimens by histological and molecular analysis. *The J Urol* 2006;176:1957-1962.
4. Skinnider BF, Amin MB. An immunohistochemical approach to the differential diagnosis of renal tumors. *Semin Diagn Pathol.* 2005;22:51-68.
5. Every AK, Beckstead J, Renshaw A, et al. Use of antibodies to RCC and CD10 in the differential diagnosis of renal neoplasms. *Am J Surg Pathol* 2000;24:203-210.
6. Stopyra G, Warhol M, Mulhaupt HAB. Cytokeratin 20 immunoreactivity in renal oncocytomas. *J Histochem Cytochem* 2001;49:919-920.
7. Delahunt B, Eble JN. Papillary renal cell carcinoma: A clinicopathologic and immunohistochemical study of 105 tumors. *Mod Pathol* 1997;10:537-544.
8. Parkkila S. An overview of the distribution and function of carbonic anhydrases in mammals. In: the carbonic anhydrases: New horizons. Chegwiddden WR, Carter N and Edwards Y; Eds. Birkhauser Verlag, Basel, Switzerland, 2000, pp76-93.
9. Pastorekova S, Parkkila S, Pastorek J, et al. Carbonic anhydrases: current state of the art, therapeutic applications and future prospects. *J Enzyme Inhib Med Chem.*2004;19:199-229.
10. Hilvo M, Tolvanen M, Clark A, et al. Characterization of CA XV, a new GPI-anchored form of carbonic anhydrase. *Biochem J* 2005;392:83-92.
11. Potter C, Harris AL. Hypoxia inducible carbonic anhydrase IX, Marker of tumor hypoxia, survival pathway and therapy target. *Cell Cycle* 2004;3:164-167.
12. Dorai T, Sawczuk I, Pastorek J, et al. Role of carbonic anhydrases in the progression of renal cell carcinoma subtypes: Proposal of a united hypothesis.
13. Gatenby RA, Gillies RJ. Why do cancers have high aerobic glycolysis? *Nat Rev Cancer.* 2004;4:891-899.
14. Graeber TG, Osmanian C, Jacks T, et al. Hypoxia mediated selection of cells with diminished apoptotic potential in solid tumors. *Nature* 1996; 329:88-91.
15. Martinez-Zaguilan R, Seftor EA, Seftor RE, et al. Acidic pH enhances the invasive behavior of human melanoma cells. *Clin Exp Metastasis* 1996;14:176-186.
16. Brand K. Aerobic glycolysis by proliferating cells: protection against oxidative stress at the expense of energy yield. *J Bioener Biomemb* 1997;29:355-364.

Automated Double Immunoenzymatic and Colorimetric In-Situ Hybridization Techniques in Evaluation of Immunoglobulin Light Chain Expression

Webber BA^{1,2} and Cohen C²

1. Laboratory Services, Veterans Administration Medical Center, Atlanta, GA, USA
2. Department of Pathology and Laboratory Medicine, Emory University, Atlanta, GA, USA

Abstract

Background: Single color immunohistochemistry for kappa/lambda is complicated by high background staining, poor sensitivity in lymphoid populations, and difficulty in assessing populations in adjacent sections. We compare two alternative commercially available automated methods for evaluating immunoglobulin light chain expression on paraffin-embedded tissue: double immunoenzyme (DIE) and colorimetric in-situ hybridization (ISH).

Design: Single sections of archived paraffin embedded tissues (Emory University, Atlanta, GA) were stained via automated DIE using novel monoclonal antibodies for kappa and lambda on a Bond™ automated system (Leica Biosystems) and compared with adjacent serial sections stained via automated ISH using pre-diluted kappa and lambda probes on a Ventana Benchmark automated stainer. Cases included 17 plasma cell dyscrasia/myeloma marrows, 1 soft tissue plasmacytoma, 3 diffuse large B cell lymphomas, 2 follicular lymphomas, 6 marginal zone lymphomas, 1 lowgrade B cell lymphoma, 1 Castleman disease, 1 benign marrow plasmacytosis, and 18 tonsillar lymphoid hyperplasias. All marrows were B5-fixed and decalcified using a hydrochloric acid (HCl) based rapid decalcifying solution, while the remaining cases were processed using formalin, B5, or B-plus fixative. Findings were correlated with previously documented flow cytometric immunophenotyping results.

Result: Correct assessment of clonality was achieved in 33 (66%) and in 28 of 50 (56%) cases by DIE and ISH, respectively. The remaining cases were indeterminate because of absent or poor quality staining. Kappa/lambda expression was only observed in plasma cells, with no reliable staining of lymphoid populations identified by either method. While fixation method had no adverse effect, a large proportion of decalcified specimens yielded non-diagnostic results because of poor quality or absent staining.

Conclusion: DIE and ISH overall are moderately effective methods for evaluating immunoglobulin light chain expression in plasma cells, but these methods demonstrate only limited success in tissues undergoing rapid, HCl-based decalcification.

Introduction

Immunoglobulin (Ig) light chain restriction is a characteristic feature of B cell neoplasia that is frequently employed in diagnosis. While flow cytometric immunophenotyping (FCI) is useful to establish B cell clonality in clinical specimens, this methodology requires fresh tissue, which occasionally is unavailable. In addition FCI may fail to identify the potentially neoplastic population, as can be seen in patchy disease, fibrotic specimens, or large cell lymphomas. In such cases, it may be necessary to assess paraffin-embedded fixed tissues to establish B cell/plasma cell clonality. In clinical practice, single color detection based immunohistochemistry (IHC) for kappa and lambda Ig light chains is the most common means to assess for light chain restriction in histologic sections. Unfortunately, single color detection based IHC is complicated by high background staining, poor sensitivity in non-plasma cell populations, and difficulty identifying particular cell populations in adjacent sections.^{1,2} Recently, alternative automated methods for evaluating kappa/lambda expression have emerged. Colorimetric in situ hybridization (CISH) using oligonucleotide probes with specificity for kappa and lambda light chain mRNA is currently available on automated platforms and theoretically lacks the background tissue staining

typically seen using IHC methods. In addition, some studies have demonstrated higher sensitivity for CISH in establishing monoclonality, even in B cell non-Hodgkin lymphomas with lower levels of light chain expression than is generally seen in plasma cell neoplasia.³⁻⁶ In addition, automated platforms capable of employing double immunoenzymatic (DIE) techniques—modifying classical immunohistochemical methods to allow simultaneous evaluation on a single slide of two cell markers in two colors, one brown (peroxidase-based) and one red (alkaline phosphatase-based) are now commercially available.

This method eliminates the need to compare staining patterns on two separate adjacent sections. With only a single slide to evaluate, the pathologist is spared the complexities associated with following cell populations on different sections, potentially improving sensitivity.⁷⁻¹⁰ In this study, we compare efficacy of an automated CISH (Ventana Benchmark automated stainer, Tucson, AZ) with an automated DIE (Bond-max Autostainer, Leica Microsystems) method for evaluating kappa/lambda expression in tissues harboring lymphoid or plasma cell lesions processed with B5 (both decalcified and non-decalcified), formalin, and B-plus fixatives.

Method

Sections of archived paraffin embedded tissues (Emory University) were stained via automated DIE using novel monoclonal antibodies for kappa (clone CH15) and lambda (clone 5H153) on a Bond (Leica Biosystems, Melbourne, Australia) automated system and compared with adjacent serial sections stained via automated CISH using pre-diluted kappa and lambda probes on a Ventana Benchmark automated stainer. Cases included both monoclonal and polyclonal plasma cell proliferations, lymphomas, and follicular hyperplasia (see Table 1). Fixation/processing methods included formalin, B5 (with and without decalcification), and B-plus (see Table 2). All marrows were decalcified with HCl-based RDO Rapid Decalcifier (Apex Engineering Products Corporation). Upon pathologist review, results were classified as κ or λ light chain-restricted, polyclonal, or indeterminate. Findings were correlated with flow cytometric immunophenotyping.

Diagnosis	No. of cases
Plasma cell dyscrasia/myeloma	17
Extramedullary plasmacytoma	1
B cell lymphoma	
Marginal zone lymphoma	4
Splenic marginal zone lymphoma	2
Follicular lymphoma	2
Diffuse large B cell lymphoma	3
Low grade B cell lymphoma, NOS	1
Polyclonal	
Benign marrow plasmacytosis	1
Castleman disease, plasma cell variant	1
Tonsillar follicular lymphoid hyperplasia	18
TOTAL	50

Table 1. Diagnoses of cases analyzed by DIE and CISH

Manner of Processing	No. of cases
Decalcified, B5-fixed	18
Non-decalcified, formalin-fixed	23
Non-decalcified, B5-fixed	6
Non-decalcified, B-plus-fixed	3

Table 2. Fixation method of cases analyzed by DIE and CISH

Results

Decalcified, B5-fixed

In the FCI confirmed plasma cell dyscrasia/myeloma cases, 12 of 17 (71%) decalcified, B5-fixed marrow cores demonstrated appropriate light chain restriction by DIE on the Leica automated platform. In the diagnostic cases, both the alkaline phosphatase-based red kappa and the diaminobenzidine-based brown lambda color labels yielded a range from weak, blush-like to strong cytoplasmic staining of plasma cells. Non-specific mild to moderate background staining was occasionally observed for both antibodies and typically was more pronounced at the tissue edge. When compared to FCI findings, no cases were erroneously

classified as the incorrect light chain restriction or as polyclonal, and all 5 cases failing to achieve correct assessment of clonality were classified as indeterminate.

By comparison, only 8 of 17 (47%) of these plasma cell neoplasia marrow cores were diagnostic for plasma cell clonality by CISH. The alkaline phosphatase blue detector stain, when visible, demonstrated a broad range of cytoplasmic plasma cell staining, from a faint blush to intense coloration. However, in six of these 8 diagnostic cases, significant portions of the slide failed to show any staining, and the diagnosis was only made based on patchy areas which were convincing for light chain restriction. Similar to the DIE method, all cases failing to achieve correct assessment of clonality were classified as indeterminate, with no results directly conflicting with FCI findings. The single marrow with polyclonal plasmacytosis was correctly classified by CISH, while DIE yielded an indeterminate result with insufficient plasma cell staining for interpretation.

Non-decalcified, Formalin-fixed

In general, non-decalcified formalin-fixed tissues demonstrated appropriate cytoplasmic Ig light chain detection in plasma cells by both DIE and CISH methods. Both methods detected light chain restriction in the soft tissue plasmacytoma and showed polyclonal patterns in the single case of plasma cell variant of Castleman disease and all 10 benign tonsillar follicular hyperplasia cases, consistent with original diagnoses. However, neither method yielded diagnostic results in lymphoma cells. Only 1 of 11 lymphoma cases (9%) showed diagnostic evidence of light chain restriction, and that was in background plasma cells expressing the same light chain by both DIE and CISH as was detected in the lymphoid population by FCI. One diffuse large B cell lymphoma was classified as indeterminate, but with focal areas noted as suspicious for faint kappa light chain expressing lymphoma cell staining by both DIE and ISH. Retrospectively, the suspicious kappa restriction was consistent with FCI findings.

Non-decalcified, B5-fixed

Performance on both DIE and CISH was similar on B5-fixed, non-decalcified tissues with no light chain detection identified on one lymphoma case and appropriate polyclonal plasma cell expression pattern in all 5 (100%) tonsillar follicular hyperplasias.

Non-decalcified, B-plus-fixed

All 3 B-plus-fixed, non-decalcified tonsils with follicular lymphoid hyperplasia showed appropriate polyclonal plasma cell staining, without any light chain detection in lymphocytes, similar to formalin and B5 fixed tissues.

Discussion

Several methods are available to establish B cell and plasma cell clonality, including FCI and molecular diagnostic studies. It is occasionally necessary to assess paraffin embedded tissue for Ig light chain expression. For such situations, single color IHC for kappa and lambda Ig light chain expression remains the most common method used in clinical practice. Unfortunately, this technique often yields suboptimal results because of high background staining and is subject to misinterpretation.^{1,2}

The advent of commercially available automated platforms simplifying otherwise cumbersome manual procedures has allowed novel detection and staining methods—such as DIE and CISH—to become realistic and affordable options currently available to the clinical laboratory. DIE employs a combination of traditional IHC techniques to assess antigen expression for two markers simultaneously on a single slide, potentially eliminating ambiguities that can arise in identifying specific cell populations in adjacent serial sections.⁷⁻¹⁰ Alternatively, CISH uses nucleic acid probes to detect target mRNA, theoretically avoiding nonspecific background extracellular labeling that can occur in IHC detection if the corresponding protein product is secreted in significant quantities.^{1, 3, 5, 11-13}

A few studies have demonstrated excellent performance of automated CISH in detecting Ig light chain restriction in both plasma cell neoplasia and non-Hodgkin lymphoma.^{3, 5} However, little attention has been paid to potential interference from use of harsh, acid-based decalcifying methods which may degrade target mRNA sequences.^{14, 15} This study demonstrated superior diagnostic sensitivity of DIE over CISH in assessment of plasma cell light chain expression in trephine biopsies which had undergone decalcification with the commercially available rapid hydrochloric acid based solution used at our institution. This

finding may be due to greater resistance of target Ig light chain protein to degradation during decalcification as compared to the corresponding target mRNA.^{14, 15} Interestingly, the method of fixation (formalin versus B5 versus B-plus) was not a differentiating factor in the performance of either of these methods, as evidenced by similar results for DIE and CISH in detecting plasma cell kappa/lambda expression in non-decalcified tissues. Also, despite reports from previous studies indicating superior performance of CISH in detecting Ig light chain expression in non-Hodgkin lymphoma, this study showed essentially no utility of either DIE or CISH in detecting kappa or lambda expression in lymphoid populations, either neoplastic or non-neoplastic. While less harsh decalcifying techniques would be likely to yield better results for CISH than were observed in this study^{14, 15}, laboratories that may be considering assessing kappa/lambda expression by CISH must be aware of these potential interfering factors. Optimization of the conditions of decalcification may be necessary for successful implementation of this technique. Laboratories should also be aware that automated DIE offers an additional alternative to traditional IHC that appears to yield less false negative staining under some decalcification conditions than CISH, while addressing some of the frustrations that plague interpretation of single color IHC.

References

- Weiss LM, Movahed LA, Chen YY, et al. Detection of immunoglobulin light-chain mRNA in lymphoid tissues using a practical in situ hybridization method. *American Journal of Pathology*. 1990;137:979-88.
- Warnke RA, Rouse RV. Limitations encountered in the application of tissue section immunodiagnosis to the study of lymphomas and related disorders. *Human Pathology*. 1985;16:326-31.
- Beck RC, Tubbs RR, Hussein M, et al. Automated colorimetric in situ hybridization (CISH) detection of immunoglobulin (Ig) light chain mRNA expression in plasma cell (PC) dyscrasias and non-Hodgkin lymphoma. *Diagnostic Molecular Pathology*. 2003;12:14-20.
- Aguilera NS, Kapadia SB, Nalesnik MA, et al. Extramedullary plasmacytoma of the head and neck: use of paraffin sections to assess clonality with in situ hybridization, growth fraction, and the presence of Epstein-Barr virus. *Modern Pathology*. 1995;8:503-8.
- Magro C, Crowson AN, Porcu P, et al. Automated kappa and lambda light chain mRNA expression for the assessment of B cell clonality in cutaneous B cell infiltrates: its utility and diagnostic application. *Journal of Cutaneous Pathology*. 2003;30:504-11.
- McNicol AM, Farquharson MA, Lee FD, et al. Comparison of in situ hybridisation and polymerase chain reaction in the diagnosis of B cell lymphoma. *Journal of Clinical Pathology*. 1998;51:229-33.
- Burg G, Kerl H, Kaudewitz P, et al. Immunoenzymatic typing of lymphoplasmacytoid skin infiltrates. *Journal of Dermatologic Surgery & Oncology*. 1984;10:284-90.
- Mason DY, Stein H, Naiem M, et al. Immunohistological analysis of human lymphoid tissue by double immunoenzymatic labelling. *Journal of Cancer Research & Clinical Oncology*. 1981;101:13-22.
- Valnes K, Brandtzaeg P. Comparison of paired immunofluorescence and paired immunoenzyme staining methods based on primary antisera from the same species. *Journal of Histochemistry & Cytochemistry*. 1982;30:518-24.
- Falini B, Abdulaziz Z, Gerdes J, et al. Description of a sequential staining procedure for double immunoenzymatic staining of pairs of antigens using monoclonal antibodies. *Journal of Immunological Methods*. 1986;93:265-73.
- Pringle JH, Ruprai AK, Primrose L, et al. In situ hybridization of immunoglobulin light chain mRNA in paraffin sections using biotinylated or hapten-labelled oligonucleotide probes. *Journal of Pathology*. 1990;162:197-207.
- Segal GH, Shick HE, Tubbs RR, et al. In situ hybridization analysis of lymphoproliferative disorders. Assessment of clonality by immunoglobulin light-chain messenger RNA expression. *Diagnostic Molecular Pathology*. 1994;3:170-7.
- Tashiro K, Ohshima K, Suzumiya J, et al. Clonality of primary pulmonary lympho proliferative disorders; using in situ hybridization and polymerase chain reaction for immunoglobulin. *Leukemia & Lymphoma*. 1999;36:157-67.
- Shibata Y, Fujita S, Takahashi H, et al. Assessment of decalcifying protocols for detection of specific RNA by non-radioactive in situ hybridization in calcified tissues. *Histochemistry & Cell Biology*. 2000;113:153-9.
- Walsh L, Freemont AJ, Hoyland JA. The effect of tissue decalcification on mRNA retention within bone for in-situ hybridization studies. *International Journal of Experimental Pathology*. 1993;74:237-41.

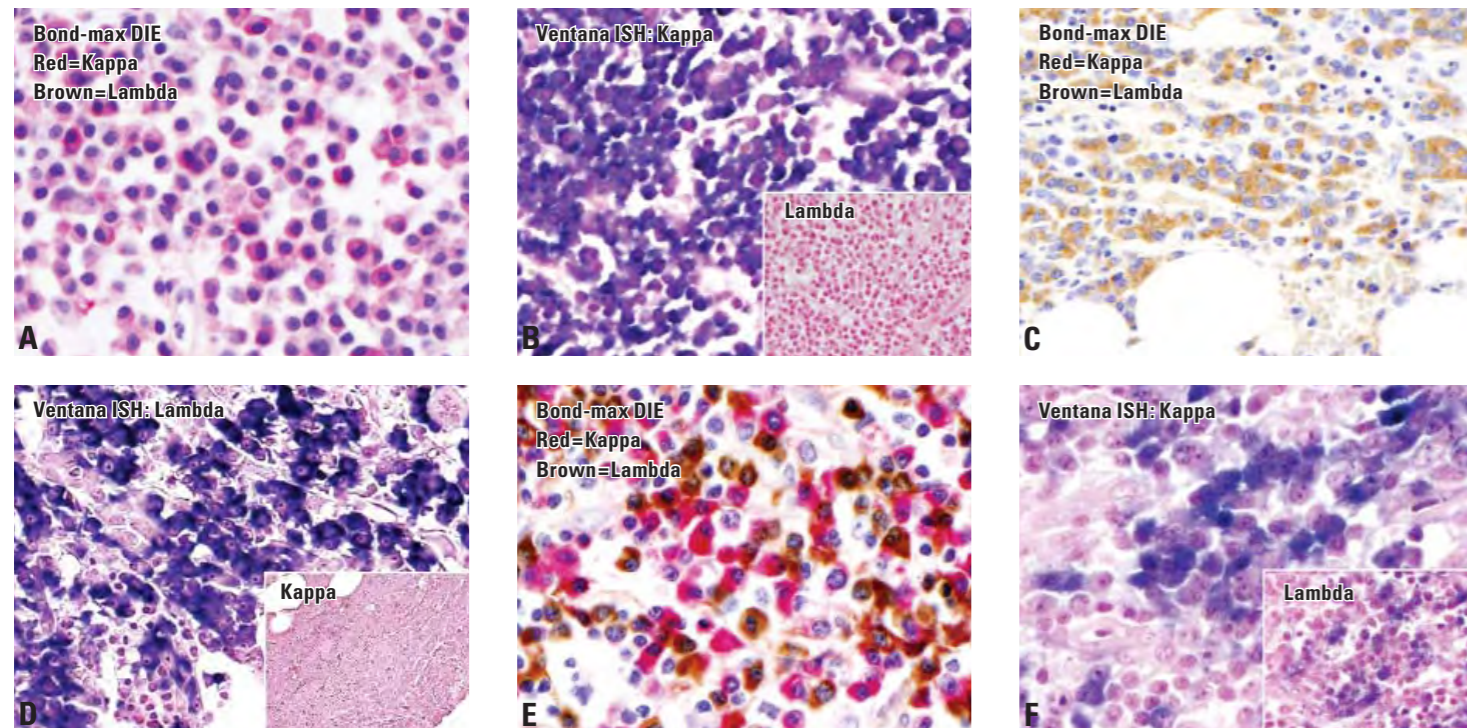


Figure 1. Plasmacytoma, Formalin-fixed, Kappa-restricted by flow cytometric immunophenotyping (FCI), appropriate Kappa staining by (A) DIE and (B) CISH. Myeloma, B5-fixed, decalcified, Lambda-restricted by FCI, appropriate Lambda staining by (C) DIE and (D) CISH. Castleman Disease, plasma cell variant, formalin-fixed, polyclonal by FCI, appropriate staining by (E) DIE and (F) CISH.

CD99: Development and Evaluation of a Novel Monoclonal Antibody for use in Manual and Automated Immunohistochemistry

Cleghorn A, Lee MJS, Doherty J, Lawson N, Walker JN, Piggott NH, Scorer PW, Pinkney M, McIntosh G

Leica Biosystems Newcastle Ltd, Balliol Business Park, Benton Lane, Newcastle upon Tyne, UK

Abstract

CD99 is a transmembrane glycoprotein which is expressed in a wide range of tissues. Although its function is not fully understood it has been implicated in a variety of cellular processes including the homotypic aggregation of the T cells, apoptosis of immature thymocytes, up-regulation of T cell receptor and MHC molecules and leukocyte diapedesis.

We have developed a novel and robust monoclonal antibody to an epitope within 101 amino acids of the N-terminal region of the human CD99 molecule. This antibody is effective in both manual and automated immunohistochemistry on formalin-fixed, paraffin-embedded tissues.

Clone PCB1 was evaluated on 329 normal and tumor tissues. Strong membranous expression was noted particularly in thymocytes, pancreatic islets and cases of Ewing's sarcoma, peripheral neuroectodermal tumors and malignant/lymphoblastic lymphomas. Clone PCB1 will be particularly useful for the differentiation of the Ewing's sarcoma family of tumors from other types of small round cell tumors.

Introduction

Ewing's sarcoma and peripheral neuroectodermal tumors (pNET) are members of a histologically similar group of tumors known as small round cell tumors of childhood and adolescence (SRCT).¹ The tumors are tan gray, often with necrotic and hemorrhagic zones. The histological pattern of SRCT ranges from uniform small round cells with round nuclei, fine chromatin and scant cytoplasm with indistinct borders to larger irregular cells with irregular nuclear contours and pseudorosettes, nesting pattern, and even spindle cells. The differential diagnosis includes tumors of neural (neuroblastomas), mesenchymal (rhabdomyosarcomas, Ewing's sarcoma, pNET, desmoplastic small round cell tumor), neuroendocrine carcinomas, acute lymphoblastic leukemia and myeloid leukemia.^{1,2} These tumors differ considerably in respect to their site of origin, etiology and prognosis. Ewing's sarcoma/pNET is the second most common bone and soft tissue sarcoma in children. It occurs more frequently in bone than extra-skeletal.

There is a male predominance. Ewing's sarcoma and pNET are diagnosed predominantly in the second decade of life.^{1,3} These tumors behave aggressively and have a tendency to metastasize rapidly.^{1,4} The Ewing's sarcoma family of tumors are associated with a reciprocal chromosomal translocation between the long arms of chromosomes 11 and 22 in approximately 85% of cases t(11;22)(q24;q12) resulting in the formation of the EWS-FLI-1 fusion gene.^{1,3,5} This aberrantly expressed fusion protein is believed to contribute to the development of Ewing's sarcoma family tumors by acting as a transcription factor which alters the expression of target genes.⁵ This translocation is not thought to be found in lymphomas, neuroblastomas or rhabdomyosarcomas.²

CD99 is a transmembrane glycoprotein, encoded by the MIC2 gene⁶ and characteristically expressed by Ewing's sarcoma and pNET. It is also detectable in acute lymphoblastic leukaemia/lymphoma, acute myelogenous leukaemia, myeloid sarcoma, synovial sarcoma and

mesenchymal chondrosarcoma. It is found in the pseudo-autosomal region of the X and Y chromosomes and is thought to escape X-chromosome inactivation. Recently the MIC2 gene has been shown to encode two distinct proteins, which are produced by alternative splicing of the CD99 transcript, and may be identified in western blots as bands of 30kDa and 32kDa.^{7,8} The two splice variants of CD99 have been shown to be differentially expressed in a variety of human cells tested.⁹⁻¹¹ They have also been shown to play opposing roles during the intercellular adhesion molecule 1 (ICAM1) mediated B cell adhesion process, with the minor truncated variant inhibiting homotypic adhesion of B cells and the major form inducing homotypic adhesion of B cells.⁹⁻¹¹ Although its function is not fully understood CD99 has also been implicated in a variety of other cellular processes including apoptosis of immature thymocytes, up-regulation of T cell receptor and MHC molecules^{6,10,12} and leukocyte diapedesis.¹³

CD99 is expressed on most human tissues including cortical thymocytes,^{1,12} pancreatic islet cells,^{1,14} Leydig and Sertoli cells,^{1,15} virtually all hematopoietic cell types (except granulocytes), peripheral blood lymphocytes,⁶ ovarian granulosa cells,^{1,7} endothelial cells,^{1,13} and basal/parabasal squamous epithelial cells.¹⁶ Although CD99 is characteristically expressed in Ewing's sarcoma, it is particularly useful in differentiating Ewing's and other small round cell tumor, particularly neuroblastoma. Expression of CD99 has been demonstrated in a wide range of tumors including lymphomas, rhabdomyosarcomas, ovarian tumors, ependymomas,^{10,16} pancreatic endocrine tumors, sex cord stromal tumors and breast carcinomas.^{1,14} The aim of this study was to develop a novel monoclonal antibody to CD99 that would give superior staining results, in terms of specificity and intensity, when compared to the existing Novocastra™ clone HO36-1.1 in both manual and automated immunohistochemistry.

Materials and Methods

Production of Soluble Human CD99 Recombinant Protein

Total RNA was extracted from washed HPB-ALL cells using an RNeasy Mini Kit (Qiagen, West Sussex, UK). For reverse transcription, 1mg of total RNA was primed with a specific primer and cDNA synthesis was carried out using the Reverse Transcription System Kit (Promega, USA) in accordance with the manufacturer's protocol.

Amplification of a 303-base pair N-terminal region of CD99 (EMBL-EBI accession number X16996) was carried out by PCR using a second CD99 specific primer and half of the reverse transcription mix as a template in a 50µL PCR reaction mix (2mM MgCl₂, 0.2mM dNTPs, 0.3mM of primer, 2.5U Taq-DNA polymerase and 1x RT transcription buffer reaction mix (Promega, USA). A total of 30 cycles of PCR (94°C/30sec, 60°C/30sec and 72°C/30sec) was performed.

A PCR product of the appropriate size was confirmed by agarose gel electrophoresis and then cloned into the pGEM-Teasy vector (Promega, USA). Clones were identified by digestion with the appropriate restriction enzymes and their identity confirmed by DNA sequencing (The Central Molecular Biology Facility, Newcastle University, UK). The cloned CD99 gene fragment was sub-cloned into the expression vector pET41b (Novagen, USA) which incorporates a GST tag on to the N-terminal end of the recombinant and also adds oligo-histidine tags to aid purification by immobilised metal ion chromatography. The resulting construct was transformed into Escherichia coli BL21 DE3 (pLysS) and protein expression was induced in cultures with the addition of isopropyl thiogalactoside (IPTG, 1mmol/L).

The CD99 recombinant fusion protein was purified by column chromatography using a Ni²⁺-IDA metal chelate resin (Generson).

Purified protein was assessed by SDS-PAGE (data not shown). When assessing hybridoma clones it was essential to use a GST screening antigen to screen out clones secreting antibody raised against the GST protein. A GST screening protein was produced using molecular recombinant technology.

Monoclonal Antibody Production

Hybridomas were generated as previously described.¹⁷ Hybridoma supernatants were screened by enzyme linked immunosorbent assay (ELISA). This involved screening the supernatants against the CD99 recombinant protein and GST to identify specific reactivity. Positive hybridoma supernatants were also screened by immunohistochemistry. Hybridomas producing CD99 antibodies were selected and clones established by limiting dilution.

Immunohistochemistry

Immunohistochemical validation was performed on a range of normal and tumor tissues using the selected mouse monoclonal CD99 antibody, clone PCB1, in conjunction with the Novolink™ Polymer Detection

System RE7140-K (250 tests). Paraffin sections, 4mm thick, were cut on to Leica Microsystems charged coated slides (S21.2113.A). To facilitate adhesion, these slides were then dried overnight at 37°C and finally baked for 1 hour at 56°C. Sections were deparaffinised in xylene and rehydrated through graded alcohols.

Heat induced epitope retrieval was performed using Epitope Retrieval Solution pH6.0 (RE7113) in a Prestige pressure cooker for 8 minutes at full pressure. Endogenous peroxidase activity was blocked by incubation for 5 min in peroxide block solution. Slides were washed in 50 mM Tris buffered saline (TBS, pH 7.6) for 5 minutes, incubated with protein block for 5 minutes and washed in TBS for a further 5 minutes. Sections were then incubated for 30 minutes at 25°C with CD99 primary antibody diluted 1:100 in IHC diluent (RE7133). Following two sequential 5 minute wash steps in TBS, sections were incubated in rabbit anti-mouse Post Primary for 30 minutes at 25°C. Two sequential 5 minute wash steps in TBS were again performed and sections incubated for 30 minutes at 25°C with Novolink Polymer. Two further sequential 5 minute wash steps in TBS were performed and bound peroxidase visualised using DAB chromogen. The DAB working solution was prepared by adding 50µL of DAB chromogen per mL of DAB Substrate Buffer. Slides were washed in water and then sections were counterstained with hematoxylin. Finally sections were dehydrated, cleared and mounted in DPX.

All scoring was carried out by senior scientists experienced in the assessment of immunohistochemical staining and tissue histology. In normal tissues, membrane staining of tissue elements was noted and the staining intensity recorded as either, negative, weak, moderate or strong. In tumor tissues, any membrane staining of tumor elements was classified as "positive" regardless of the staining intensity.

Automated Immunohistochemistry

Clone PCB1 was shown to be effective on the Leica automated Bond™ system using Bond™ Epitope Retrieval Solution 1 (AR9961) and Bond™ Polymer Refine Detection (DS9800). Protocol F applied epitope retrieval for 20 minutes, incubation with clone PCB1 for 15 minutes, incubation with Post Primary for 8 minutes, Polymer for 8 minutes, DAB for 10 minutes and hematoxylin for 5 minutes. Staining was unaffected by the position of the peroxidase block step in the protocol.

External Evaluation

Clone PCB1 was evaluated by Dr Korinna Jöhrens at the Charité - Universitätsmedizin Berlin, Germany.

Results

Normal Tissues

Table 1 shows the staining for CD99 in normal tissues. Clone PCB1 detected the CD99 protein in a variety of tissues including lymphocytes, vessel endothelium and basal epithelia of tonsil and pancreatic islets (Figure 1). (Total number of cases stained = 80).

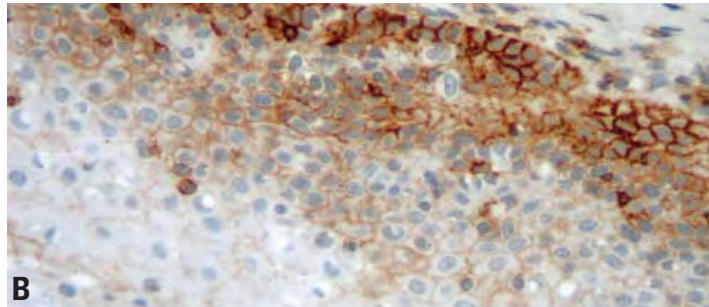
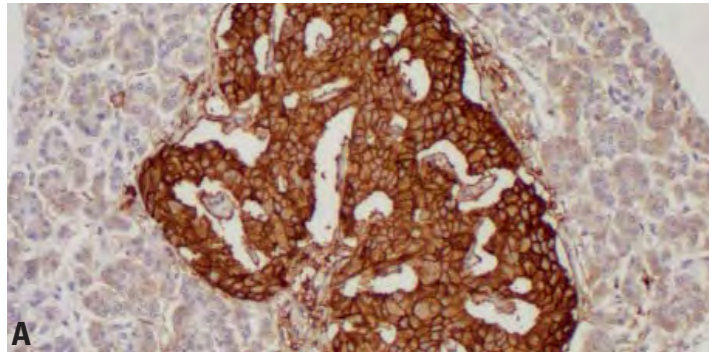


Figure 1. Immunohistochemical staining for CD99 using clone PCB1 on A) pancreas and B) tonsil (original magnification x200). Manual staining of paraffin section.

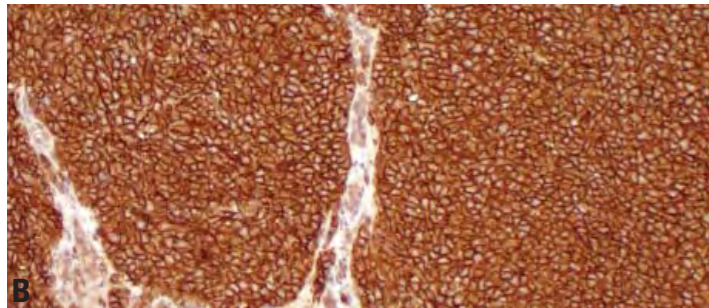
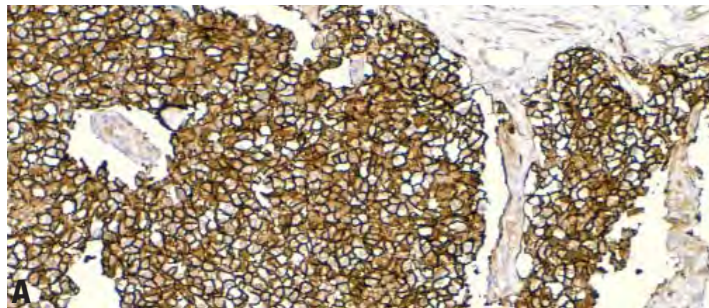


Figure 2. Immunohistochemical staining for CD99 using clone PCB1 on A) Ewing's sarcoma (original magnification x200) and B) pNET (original magnification x200). Bond™ automated system staining of paraffin sections.

Abnormal Tissues

Clone PCB1 detected the CD99 protein in 31/40 soft tissue tumors and sarcomas (Table 2), where staining was particularly noted in pNET and Ewing's sarcoma (Figure 2). Clone PCB1 also stained 19/51 hematological malignancies (Table 3), 14/68 lung tumors (Table 4) and 28/34 prostate tumours (Gleeson grade 6-9) (Table 5). (Total number of cases stained = 247).

Table 1. Immunostaining for CD99 in Normal Tissues

Tissue	Staining Results
Adrenal	Negative
Appendix	Strong membrane staining of epithelium
Bone marrow	Moderate membrane staining of a subset of lymphocytes
Bowel, large	Strong membrane staining of epithelium
Bowel, small	Strong membrane staining of epithelium
Brain, cerebellum	Strong staining of white matter
Breast	Strong membrane staining of occasional cells in glandular and ductal epithelium
Cervix	Strong membrane staining of basal epithelium
Esophagus	Moderate membrane staining of epithelium
Kidney	Strong membrane staining of glomerular capillaries
Liver	Strong membrane staining of hepatocytes
Lung	Strong membrane staining of bronchial epithelium
Muscle, skeletal	Negative
Myocardium	Negative
Ovary	Moderate membrane staining in stromal cells
Parathyroid	Negative
Pancreas	Strong membrane and cytoplasmic staining of islets of Langerhans and occasional acinar epithelial cells
Pituitary	Moderate membrane and cytoplasmic staining of pituicytes
Prostate	Strong membrane staining of acinar epithelium
Salivary Glands	Moderate membrane staining of glandular and ductal epithelium
Spleen	Moderate membrane staining of splenocytes in white pulp
Skin	Strong membrane staining of basal epithelium
Stomach	Strong membrane staining of epithelium and gastric glands
Testis	Strong membrane and cytoplasmic staining of tubules
Thymus	Strong membrane staining of thymocytes
Thyroid	Strong membrane staining of occasional follicular epithelial cells
Tonsil	Strong membrane staining of basal epithelium
Umbilical cord	Strong membrane staining of mesothelium
Uterus (myometrium)	Weak/moderate membrane staining of myometrial stromal cells

In positive tissues peripheral lymphocytes and vessel endothelium were positive (where present) with clone PCB1, all other tissue elements were negative.

Table 2. Immunostaining for CD99 in Soft Tissue Tumors and Sarcomas

Tissue	IHC Positivity
pNET	15/17
Chordoma	8/10
Synovial sarcoma	3/5
Sarcoma epithelioides	2/3
Ewing's sarcoma	1/1
Desmoplastic small round cell tumor	1/1
Clear cell sarcoma	1/1
Malignant rhabdoid tumor	0/1
Alveolar soft part sarcoma	0/1

Table 3. Immunostaining for CD99 in Hematological Malignancies

Tissue	IHC Positivity
Diffuse large B cell lymphoma	1/9
Follicular lymphoma	2/6
Hodgkin's lymphoma	1/5
Anaplastic large cell lymphoma	2/3
Peripheral T cell lymphoma	2/3
MALT-lymphoma	2/2
T lymphoblastic lymphoma	1/1
Marginal zone lymphoma	0/1
Mantle cell lymphoma	0/2
Non-Hodgkin's lymphoma (unclassified)	0/2
Burkitt's lymphoma	0/2
NK/T cell lymphoma	0/2
Unspecified lymphoma	7/13

Table 4. Immunostaining for CD99 in Lung Tumors

Tissue	IHC Positivity
Adenocarcinoma	6/23
Squamous cell carcinoma	5/20
Small cell carcinoma	1/8
Large cell carcinoma	1/2
Atypical carcinoma	1/2
Papillary adenocarcinoma	0/8
Bronchioalveolar carcinoma	0/2
Giant cell carcinoma	0/2
Non-small cell carcinoma	0/1

Table 5. Immunostaining for CD99 in Miscellaneous Tumors

Tissue	IHC positivity
Prostate - Gleeson grade 6-9	28/34
Pancreas - duct adenocarcinoma	1/19
Pancreas - islet cell carcinoma	0/2
Squamous cell carcinomas (various locations)	1/10
Liver - hepatocellular carcinoma	2/2
Liver - cholangiocarcinoma	0/2
Ovary - transitional cell carcinoma	0/2
Ovary - mucinous cystadenocarcinoma	1/1
Ovary - clear cell carcinoma	0/1
Colorectal -adenocarcinoma	1/3
Stomach - adenocarcinoma	1/2
Thyroid - papillary carcinoma	0/2
Thyroid - follicular carcinoma	0/2
Kidney - clear cell RCC	0/2
Brain - glioblastoma	0/1
Brain - glioma	0/1
Breast - ductal carcinoma	0/2

Novocastra™ NCL-CD99 (clone H036-1.1)

Immunohistochemical staining using our existing Novocastra™ product, NCL-CD99 (clone H036-1.1), highlighted non-specific cross-reactive staining in several tissues.

Western blotting also highlighted that in addition to a weak band at the correct molecular weight (32kDa), clone H036-1.1 also produced an additional strong band at a higher molecular weight (IHC and blotting data not shown). Western blotting confirmed that clone PCB1 produced a single band at 32kDa (data not shown).

Conclusion

We have developed a novel monoclonal antibody to CD99 for use in formalin-fixed, paraffin-embedded tissue immunohistochemistry. NCL-L-CD99-187, clone PCB1, was shown to be effective at a dilution of 1:100 using Heat Induced Epitope Retrieval solution pH 6 and the Novolink Polymer Detection System. Staining was unaffected by the position of the peroxidase block step in the protocol or the use of TBS or PBS-based diluents and wash buffers. The antibody is also effective on the automated Bond system using Bond Epitope Retrieval Solution 1 (AR9961) and Bond Polymer Refine Detection (DS9800).

Clone PCB1 gives superior immunohistochemical staining results, in terms of specificity and intensity, in comparison to our existing Novocastra clone H036-1.1 in both manual and automated immunohistochemistry. It will be an important immunological tool for the differentiation of Ewing's sarcoma and other peripheral neuroectodermal tumors from other types of small round cell tumor.

References

1. Ambros I, Ambros P, Strehl S, et al. MIC2 is a specific marker for Ewing's sarcoma and peripheral primitive neuroectodermal tumors. *Cancer*. 1991; 67:1886-1893.
2. Fellingner E, Garin-Chesam P, Triche T, et al. Immunohistochemical analysis of Ewing's sarcoma cell surface antigen p30/32. *American Journal of Pathology*. 1991; 139(2):317-325.
3. Bernstein M, Kovar H, Paulussen M, et al. Ewing's sarcoma family of tumors: current management. 2006; 11:503-519.
4. Devoe K and Weidner N. Immunohistochemistry of small round cell tumors. *Seminars in diagnostic pathology*. 2000; 17(3):216-224.
5. Riggi N and Stamenkovic I. The biology of Ewing's sarcoma. *Cancer Letters*. 2007; 254:1-10.
6. Gil M, Lee M, Seo J, et al. Characterization and epitope mapping of two monoclonal antibodies against human CD99. *Experimental and Molecular Medicine*. 2002; 34(6):411-418.
7. Choi Y, Kim H, Ahn G. Immunoexpression of inhibin a subunit, inhibin/activin bA subunit and CD99 in ovarian tumors. *Archives of Pathology and Laboratory Medicine*. 2000; 124:563-569.
8. Fellingner E, Garin-Chesa P, Su S, et al. Biochemical and genetic characterization of the HBA71 Ewing's sarcoma cell surface antigen. *Cancer Research*. 1991; 51:336-340.
9. Lee H, Kim B, Hahn J, et al. Functional involvement of src and focal adhesion kinase in a CD99 splice variant-induced motility of human breast cancer cells. *Experimental and Molecular Medicine*. 2002; 34(3):177-183.

10. Jung K, Park W, Bae Y, et al. Immunoreactivity of CD99 in stomach cancer. *Journal of Korean Medical Sciences*. 2002; 17:483-489.
11. Hahn J, Kim M, Choi E, et al. CD99 (MIC2) regulates the LFA-1/ICAM-1-mediated adhesion of lymphocytes, and its gene encodes both positive and negative regulators of cellular adhesion. *Journal of Immunology*. 1997; 159(5):2250-2258.
12. Choi E, Park W, Jung K, et al. Engagement of CD99 induces up-regulation of TCR and MHC class I and II molecules on the surface of human thymocytes. *The Journal of Immunology*. 1998; 161:749-754.
13. Schenkel A, Mamdouh Z, Chen X, et al. CD99 plays a major role in the migration of monocytes through endothelial junctions. *Nature Immunology*. 2002; 3(2):143-150.
14. Goto A, Niki T, Terado Y, et al. Prevalence of CD99 protein expression in pancreatic endocrine tumors (PETs). *Histopathology*. 2004; 45:384-392.
15. Verakorva E, Laato M, Pollanen P. CD99 and CD106 (VCAM-1) in human testis. *Asian Journal of Andrology*. 2002; 4(4):243-248.
16. Mahfouz S, Aziz A, Gabal S, et al. Immunohistochemical study of CD99 and EMA in ependymomas. *Medscape Journal of Medicine*. 2008; 10(2): 41.
17. Rees ML, Marshall I, McIntosh GG, et al. Wild-type estrogen receptor beta expression in normal and neoplastic paraffin-embedded tissues. *Hybridoma and Hybridomics*. 2004; 23(1):11-18.

Disclaimer

Unless otherwise stated all references quoted refer to data on CD99 derived from established scientific publications involving various antibodies and techniques and do not refer to IHC staining expression directly attributable to NCL-L-CD99-187.

R&D Reflections

Gary McIntosh, Novocastra Antibody Research and Development Manager

Leica Biosystems Newcastle Ltd

Since our last edition of reAGENTS we have continued to add new antibodies to our range of Novocastra™ concentrates and expand our range of Bond™ ready-to-use primary antibodies. They say that a picture is worth a thousand words and that is certainly true of the antibodies that we have released throughout the past year. As with so many of the antibodies in the Novocastra portfolio, all of these antibodies have been generated 'in-house' by our own molecular biology and hybridoma development teams.

Our last issue of reAGENTS (Volume 02, Issue 01) referred to the up and coming release of the eagerly awaited new monoclonal antibodies to CD19 (clone BT51E), CD30 (clone JCM182), Akt (phosphorylated) (clone LP18) and Oct3/4 (clone N1NK) and I am delighted to confirm that these became available at the end of 2008 along with Carbonic Anhydrase IX (clone TH22), N-Cadherin (clone IAR06), Immunoglobulin A (clone N1CLA) and Minichromosome Maintenance Protein 6, (clone KAT82). All of these antibodies are available as liquid concentrates and are effective in tissue immunohistochemistry on formalin-fixed, paraffin-embedded (FFPE) tissue sections.

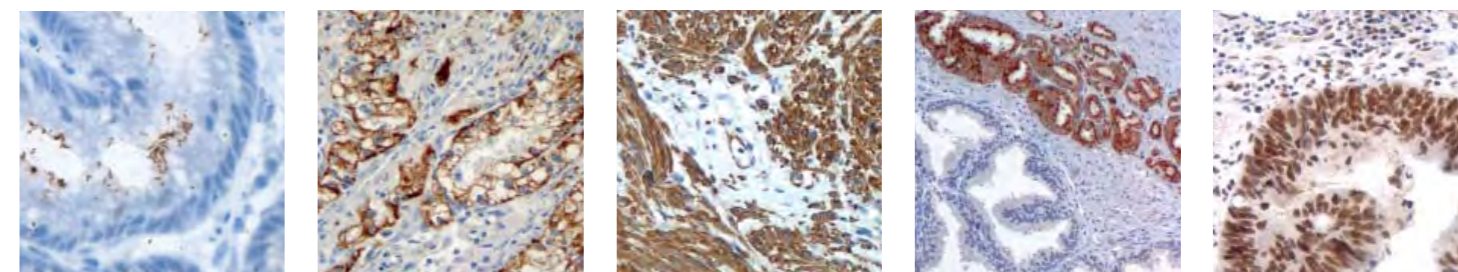
In 2009 and 2010, we released an additional fifteen new monoclonal antibodies. These include antibodies that we have developed to supersede those already in our portfolio. Our new antibody to CD99 (clone PCB1) provides a significant improvement in terms of specificity and sensitivity over our previous monoclonal antibody clone HO36-1.1 (see preceding article in this edition). Our new Calcitonin monoclonal antibody (clone CL1948) also provides the advantage over our existing polyclonal antibody, NCL-CALp, of strong, specific staining without the non-specific background levels associated with the polyclonal antibody.

Similarly, our new Kappa Light Chain (clone CH15) and Lambda Light Chain (clone SHL53) monoclonals provide the same advantage over our existing polyclonal antibodies. Our new Muscle Specific Actin antibody (clone SC28) is more sensitive in detecting soft tissue and muscle tumours than our current clone HHF35. We are also delighted to announce the release our new monoclonal antibody to *Helicobacter pylori* (clone ULC3R). This is yet another product that we have developed to supersede an existing product in our range. This antibody gives more defined staining of *H.pylori* bacteria than NCL-HPp and unlike its polyclonal counterpart it does not cross-react with *Campylobacter jejuni*.

In releasing our new Mismatch Repair Protein PMS2 (clone M0R4G) we have completed the quartet of Mismatch Repair Protein antibodies with it complimenting our existing MSH2 (clone 25D12), MLH1 (clone ES05) and MSH6 (clone PU29). Further important additions to the Novocastra range of antibodies include MUM-1 (clone EAU32), AMACR p504s, (clone EPMU1, not available in the USA due to patent restrictions), Inhibin Alpha (clone AMY82) and Immunoglobulin G (clone RWP49). The latter of which completes a quartet of novel Ig monoclonal antibodies offering excellent specificity and a competitive working dilution.

New and unique antibodies for FFPE tissue immunohistochemistry include those to Folate Receptor Alpha (clone BN3.2),¹ Hypoxia Inducible Gene 2 Protein (clone HX34Y) and Folylpolyglutamate Synthetase, (clone AS2) and we are seeing significant research interest in the use of these antibodies with a view to a clinical application.

For more information on these antibodies please contact your local sales representative.



Immunohistochemical staining using novel antibodies to: *H.pylori*, clone ULC3R, on *H.pylori* infected tissue (x1000 original magnification); HIG2, clone HX34Y, on clear cell renal cell carcinoma (x400 original magnification); MSA, clone SC28, on leiomyosarcoma (x400 original magnification); AMACR (p504s), clone EPMU1, on prostate adenocarcinoma (x200 original magnification); PMS2, clone M0R4G, on colon cancer (x400 original magnification). Paraffin sections.

References

1. Smith AE, Pinkney M, Piggott NH et al. A novel monoclonal antibody for detection of folate receptor alpha in paraffin-embedded tissues. *Hybridoma*. 2007; 26(5): 281-288.

Leica Microsystems - an international company with a strong network of customer services

Novocastra reagents are available through the following offices:

Asia/Pacific

Sales orders/customer support Aus 1800 246 797

Sales orders/customer support NZ 0800 400 589

Europe/Middle East/Africa

Sales orders/customer support UK 0800 298 2344

Sales orders/customer support ROI 1800 242 612

Sales orders/customer support EU +44 191 215 4242

North America

Sales orders/customer support USA 800 248 0123

Sales orders/customer support Canada 800 205 3422

Copyright

All material in reAGENTS, including the layout, images, text and other information is the property of Leica Biosystems Newcastle Ltd, its affiliates, related companies and licensors and is protected by the law of copyright, international copyright conventions and other intellectual property laws.

You may not reproduce, distribute, modify, publish, transmit, create works from, sell or license all or any part of the material in reAGENTS without the prior written permission of Leica Microsystems Ltd or its licensors, except as otherwise permitted under applicable law. You may not use, alter or remove any trade mark, copyright or other proprietary notice appearing in or on the material in reAGENTS.

Disclaimer

The ideas and opinions expressed by the authors of articles published in reAGENTS are not necessarily those of Leica Biosystems Newcastle Ltd. Leica Biosystems Newcastle Ltd does not warrant or assume any liability or responsibility for the accuracy, completeness, quality, usefulness, reliability, availability or non-infringement of any information, apparatus, product, or process published in reAGENTS.

Publication of an advertisement for a product in reAGENTS is not an endorsement by Leica Biosystems Newcastle Ltd of the product or the manufacturer's claims. Users should contact the manufacturer with any questions about the features or limitations of any products advertised in reAGENTS.

Leica Biosystems Newcastle Ltd does not accept any liability or responsibility for any loss or injury and/or damage to persons or property arising out of or related to any use or reliance on any information, apparatus, product, or process published in reAGENTS. ReAGENTS is intended to provide users with information to better understand the field of histopathology and diagnosis of disorders and it is not the intention of Leica Biosystems Newcastle Ltd to provide medical, scientific or technical advice. The specific use or reliance on any information, apparatus, product, or process published in reAGENTS is the professional responsibility of the health care or other advisor, supplier or provider.

Some medical devices published in reAGENTS have regulatory clearance for limited use in restricted research settings. It is the professional responsibility of the health care or other advisor, supplier or provider to ascertain the regulatory status, in the country of use, of each medical device planned for use in their clinical practice.